Pedro Miguel Carvalho Durão

Licenciado em Biologia

The role of *fu2* gene in cell competition in *Drosophila melanogaster*

Dissertação para obtenção do Grau de Mestre em
Genética Molecular e Biomedicina

Orientador: Professor Doutor Eduardo Lampaya Moreno,
Fundação Champalimaud

Co-orientador: Doutora Catarina Brás-Pereira, Fundação
Champalimaud

Júri:

Presidente: Profesora Doutora Paula Gonçalves
Arguente: Doutor Carlos Ribeiro
Vogal Professor Doutor Eduardo Moreno

FACULDADE DE
CIÊNCIAS E TECNOLOGIA
UNIVERSIDADE NOVA DE LISBOA

Setembro, 2018

Faculdade de Ciências e Tecnologia da Universidade Nova de Lisboa

Pedro Miguel Carvalho Durão

Licenciado em Biologia

The role of *fu2* gene in cell competition in *Drosophila melanogaster*

Dissertação para obtenção do Grau de Mestre em
Genética Molecular e Biomedicina

Orientador: Professor Doutor Eduardo Lampaya Moreno, Fundação Champalimaud

Co-orientadora: Doutora Catarina Brás-Pereira, Fundação Champalimaud

Trabalho experimental desenvolvido na
Fundação Champalimaud – Champalimaud Centre for the Unknown

Setembro 2018

The role of *fu2* gene in cell competition in *Drosophila melanogaster*

Acknowledgments

First, I would like to thank my supervisor, Dr. Eduardo Moreno, for giving me the opportunity to work in a completely new model for me and in a such interesting subject as cell competition.

A deep thank you to my Co-supervisor, Catarina Brás-Pereira, who taught me how to think critically about my experiments and guided me throughout this project and without whom this project would not be possible. Thank you for all your patience and help Catarina.

To the CCU platforms, specially the MTTP thank you for helping me to improve my molecular biology skills. A special thanks to Raquel Tomás, from MTTP, for all her patience about my doubts and for always having a kind word to tell me in the most stressful moments.

I would also like to thank to all members in the lab for the support and help and for making the lab such a good place to work. A special thanks to Inês Silva who helped me a lot in my first steps with fly work and throughout the project.

To Mariana Velez, Carmo Soares, João Martins and Catarina Costa, thank you for your unwavering support and for cheering me up when I needed the most. You guys are amazing.

Also, thanks to all the people I had the pleasure to meet during the last year: Isahak Saidi, Denise Camacho, Sara Júlio, Miguel Pinto and Ana Queirós.

Um obrigado muito especial aos amigos que me acompanham desde o ensino secundário e que me ajudam a crescer todos os dias: António Santos, Mariana Pereira, Ana Costa e Miguel Bastos.

Finalmente, gostaria de agradecer aos meus pais e avós por todo o apoio familiar e por nunca duvidarem das minhas capacidades. Sem vocês, isto não seria possível.

Resumo

A competição celular é um processo através do qual células menos adaptadas (células perdedoras) são eliminadas por células circundantes mais competitivas (células vencedoras). Este mecanismo homeostático potencia o correto desenvolvimento do animal, assegurando o estado geral dos tecidos animais.

Em *Drosophila melanogaster*, as células exibem informação sobre o seu estado via differentes isoformas da proteína transmembranar Flower (Fwe). Células epiteliais sub-ótimas são detetadas e eliminadas por apoptose, porque expressam a isoforma Fwe^{lose} , enquanto células mais vigorosas expressam a isoforma Fwe^{ubi}, a isoforma vencedora. O código Fwe é, portanto, um indicador de aptidão que permite a competição direta das células e a discriminação entre células vencedoras e perdedoras. Em adição ao código Fwe, o laboratório também identificou genes sobre-regulados cedo em células perdedoras, vencidas por células vencedoras que sobre-expressam *dMyc*, comportando-se como supercompetidoras. Um destes genes é *fu2*, que codifica um fator nuclear com domínios de dedos-de-zinco. Foi mostrado que *fu2* é sobre-expresso em células sub-ótimas.

O objetivo do projeto é determinar se *fu2* é requerido para a eliminação de células em diferentes contextos de competição celular. Para tal, feramentas moleculares e moscas transgénicas foram geradas para avaliar a necessidade de *fu2* para a eliminação de células perdedoras em contextos como a doença de Alzheimer ou a eliminação neuronal.

Em relação ao contexto de Alzheimer, os resultados foram inconclusivos, uma vez que diferentes linhas de RNAi utilizadas para reduzir a expressão de *fu2* revelaram diferentes resultados. Adicionalmente, no contexto de eliminação neuronal, não foi possível analisar a função de *fu2* , visto a perda do marcador de fitness celular *azot* (*azot* KO) não revelou a redução esperada em morte celular quando comparado com uma retina de tipo selvagem (w^{1118}). Por fim, foi mostrado que as moscas *fu2* knockout são viáveis em homozigotia.

A geração de novas ferramentas durante este projeto irá permitir clarificar os resultados obtidos avaliar o papel de *fu2* na doença de Alzheimer, durante o desenvolvimento normal (eliminação neuronal) e noutros contextos de competição celular (dependentes de *fwe*).

Palavras-Chave: Competição celular; *fu2*; ferramentas moleculares; doenças de Alzheimer; eliminação neuronal.

Abstract

Cell competition is a process by which less adapted cells (loser cells) are eliminated by surrounding, more competitive cells (winner cells). This homeostatic mechanism potentiates the correct animal development and ensures overall fitness of animal tissues.

In *Drosophila melanogaster*, cells display information about their fitness state via different spliced isoforms of the transmembrane protein Flower (Fwe). Suboptimal epithelial cells are detected and eliminated by apoptosis because they express Fwe^{Lose} isoforms, whereas more vigorous cells express Fwe^{ubi} isoform, the winner isoform. Fwe code is, thus, a fitness indicator that allows direct cell competition and the discrimination between winner and loser cells. In addition to the Fwe code, Moreno's team also identified early upregulated genes in loser cells that are outcompeted by *dMyc*-overexpressing winner cells, which behave as supercompetitors. One of these genes is *fu2* which encodes a nuclear factor with Zinc-finger domains.

The goal of the project is to determine if *fu2* is required for cell elimination in different cell competition contexts. To do so, molecular tools and transgenic flies were generated to assess the requirement of *fu2* for loser cell elimination in contexts such as in Alzheimer's disease and during the neuronal culling process.

Regarding the Alzheimer's disease context, the results were inconclusive, as different lines of RNAi used to downregulate the expression of *fu2* gave different results. Additionally, in the neuronal culling context, it was not possible to analyze the function of *fu2*, since the loss of the fitness marker *azot* (*azot* KO) did not show an expected reduction in cell death when compared with a wild-type retina (w^{1118}). Finally, it was shown that *fu2* knockout flies are homozygous viable.

The generation of new tools during this work will allow to clarify the results obtained and to evaluate the role of *fu2* in Alzheimer's disease, during normal retina development (neuronal culling) and in other cell competition (*fwe*-dependent events) contexts.

Keywords: Cell competition; *fu2*; molecular tools; Alzheimer's disease; neuronal culling.

CONTENTS

List of Figures

List of Tables

List of abbreviations

Aβ – Amyloid-β
APF – after pupae formation
APP- Amyloid precursor peptide
bp – base pairs
brk - brinker
CRISPR – Cas9 – Clustered Regularly Interspaced Short Palindromic Repeats – CRISPR associated protein 9
crRNA – CRISPR RNA
DAPI - 4′,6-diamidino-2-phenylindole
Dcp-1 – Death caspase-1
dMyc – *Drosophila* myc *dpp* – decapentaplegic DSB – Double strand break
e. g. – *exempli gratia*
Elav - Embryonic Lethal Abnormal Vision
FISH – Fluorescence *in situ* hybridization
fwe – *flower*
GA – Gibson Assembly
gDNA – Genomic DNA
GMR – Glass Multiple Reporter
HA-tag – *Human influenza* hemagglutinin-tag
HDR – Homology directed repair
i.e. – *id est*
Indels – Insertions/Deletions
JNK - c-Jun N-terminal kinase
KO – Knockout
M - Minute
ME – Main epithelium
MTTP – Molecular and Transgenic Tools Platform
M/+ - Minute heterozygous mutant
ng – nanograms
NHEJ – Nonhomologous end joining
nos – nanos
PAM – Protospacer domain
PBS – Phosphate-buffered saline
PBS-T – Phosphate-buffered saline -Tripton
PCR – Polymerase chain reaction
PE – Peripodial epithelium
ROI – Region of Interest
RT – Room Temperature
sgRNA – small guide RNA
SNP – Single nucleotide polymorphism SPARC – Secreted Protein Acidic and Rich in Cysteine
ssDNA – Single stranded DNA
Ta – Annealing temperature
TFIIIA – Transcription factor IIIA
tracrRNA – trans-activating crRNA
tRNA – Transfer RNA
TSS – Transcription start site
TUNEL – Terminal deoxynucleotidyl transferase dUTP nick end labeling
UAS – Upstream activation sequence
Vta1 – Vps20-associated 1
WT - Wild Type
5'HA – 5' Homology Arm
3'HA – 3' Homology Arm

1- Introduction

1.1 - Cell competition

Since 1859, when Charles Darwin proposed the theory of natural selection in "The Origin of the Species", the understanding of organism's development is based on the "survival of the fittest". However, the original theory did not consider tissue development, as argued by the zoologist Wilhem Roux, in 1881. When Darwin's theory is applied to the cellular level, it becomes clear that cells also need to compete among themselves for space and limited resources. The result of the cellular competition is the elimination of cells with deleterious mutations and the survival and proliferation of the fittest (Moreno and Rhiner, 2014). This process is known as cell competition and it requires the presence of fitter cells, termed "winner cells" which outcompetes viable sub-optimal cells, termed "loser cells". The loser cells die by apoptosis and their cellular debris are engulfed (Lolo et al., 2013). Due to the fact that the expansion of winner cells occurs at the expense of the loser cells, the total number of cells in the tissue is preserved (Rhiner et al., 2010). Cell competition is an homeostatic mechanism designed to eliminate cells that, for some reason, are considered unfit and can harm the tissues and, consequently, the whole organism (Morata and Ballesteros-Arias, 2015). This process is conserved across species, from flies to mammals, and it may occur in different organs, during different developmental stages. For example, in flies, cell competition may occur in the wing imaginal discs or in the ovary. As for the mammalians, cell competition was shown to happen during embryo development and also in the adult thymus (Moreno and Rhiner, 2014).

Cell competition was firstly discovered in 1970, in the wing imaginal disc of *Drosophila melanogaster* (*Drosophila*), due to experiments performed with the purpose of analysing the phenotype of *Minute* mutations. *Minute* genes (*M*) encode a group of ribosomal proteins, and are, thus, involved on the synthesis of cellular components (cellular anabolism). Mutations on these genes were shown to be homozygous lethal, which is explained by the impossibility to produce proteins. However, heterozygous *Minute* mutant flies (*M*/+) were shown to be viable, though a very distinct phenotype is observed (prolonged development, short and thin bristles and decrease in fertility and viability). To date, at least 60 different *Minute* loci have been genetically identified (Marygold et al., 2007; Morata and Ballesteros-Arias, 2015; Moreno, 2008). Cell competition was discovered due to its role in the elimination of *M*/+ clones in a wild-type (WT) background. *M*/+ cells require more time to divide than WT cells and, because of this, they are considered unfit cells and die through c-Jun N-terminal kinase (JNK) pathway (Morata and Ripoll, 1975; Moreno et al., 2002).

1.1.1 – General concepts of cell competition

In general terms, cell competition is a process that can be divided in three simple steps: (1) differences in cell fitness occur, turning fit cells into "winners" and less fit, but viable, cells into "losers"; (2) then the difference in fitness status is perceived by the cells and, (3) depending on the type of cell, i. e, "winner" or "loser", they will proliferate or die, respectively (Figure 1.1 A) (Di Gregorio et al., 2016). There is,

however, a particular mechanism of cell competition, associated with cancer development, known as supercompetition (Figure 1.1 B). In this scenario, mutations acquired by some cells improve its fitness and proliferative capacity, instead of decreasing it, turning them into supercompetitors. These supercompetitors are capable of eliminating WT neighbouring cells (Levayer and Moreno, 2016; Merino et al., 2016). There have been described several genes involved in the supercompetiton process. In *Drosophila*, the most extensively studied is the proto-oncogene *Drosophila Myc* (*dMyc*), encoding for a transcription factor that regulates cell growth and ribosome biogenesis (Gogna et al., 2015). Cells with higher levels of *dMyc* (supercompetitors) outcompete adjacent cells expressing normal levels of *dMyc* (WT cells) (Moreno, 2008; Rhiner et al., 2010).

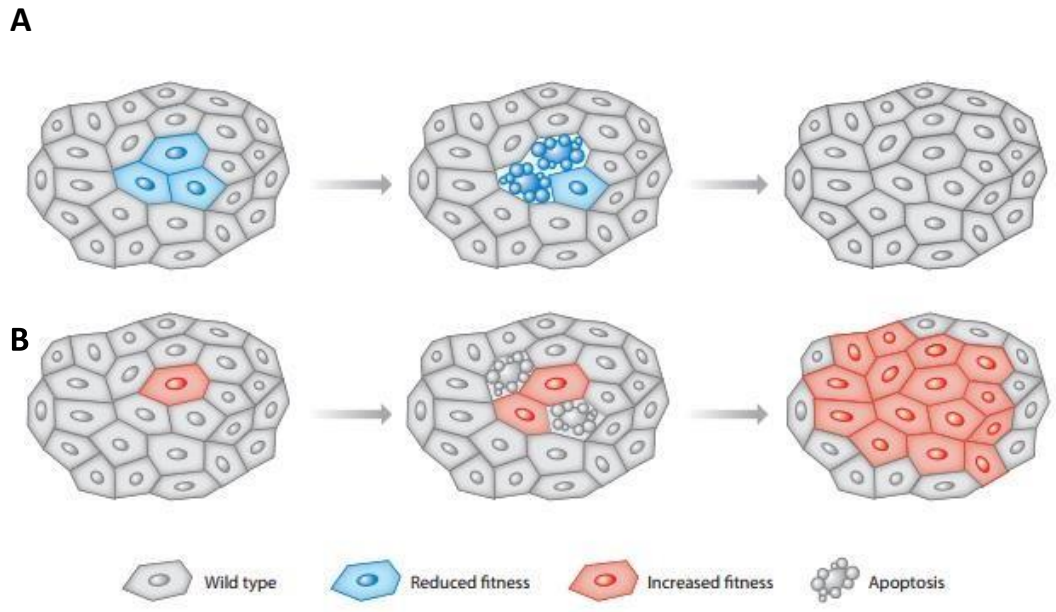

Figure 1.1 – Mechanisms by which cell competition occurs. (A) General mechanism of cell competition. When loser cells are surrounded by winner cells, apoptosis is triggered in the loser cells. Meanwhile, a compensatory proliferation occurs in winner cells, to substitute the losers. (B) Supercompetition mechanism. Cells acquire certain mutations and become more fit than WT cells, resulting in the elimination of the latter. Consequently, winner cells (supercompetitors) proliferate and can even invade other tissues. Adapted from (Clavería and Torres, 2016)

To date, three types of cell competition are described:

- Competition for survival factors – this type of cell competition was first identified in the wing imaginal discs of *Drosophila* upon the induction of *Minute* mutations. These mutated cells present a decrease in the Decapentaplegic (Dpp) signalling pathway, which is reflected in a lower proliferative capacity, when compared to the neighbouring cells. Dpp is a survival factor, involved in cell proliferation. The lack in Dpp transduction signal triggers the expression of *brinker* (*brk*), a growth repressor, which will, in turn, activate JNK apoptosis pathway (Figure 1.2 A) (Moreno et al., 2002). Currently, other survival factors, such as Wingless, were shown to induce the same type of cell competition (Vincent et al., 2011).

- Fitness comparison – through this pathway, cells report their relative fitness to the vicinity, by exposing a specific protein in the outer surface of the cellular membrane (Figure 1.2 B) (Clavería

and Torres, 2016). This protein is known as Flower, a transmembrane protein that will be later described. Fitness comparison requires cell-cell contact, and it is crucial for embryonic development and adult homeostasis.

- Mechanical constraints – cells can also respond to physical forces, using mechanical responsive sensors, which are molecules involved in the transduction of a physical signal into a biochemical one. In this type of cell competition, the sensitivity to tissue crowding determines the cellular fitness status. Compression stress induced by winner cells provokes the increase of cell density, leading to loser cell elimination. Thus, loser cells are less resistant to mechanical-induced elimination (Figure 1.2 C) (Brás-Pereira and Moreno, 2018).

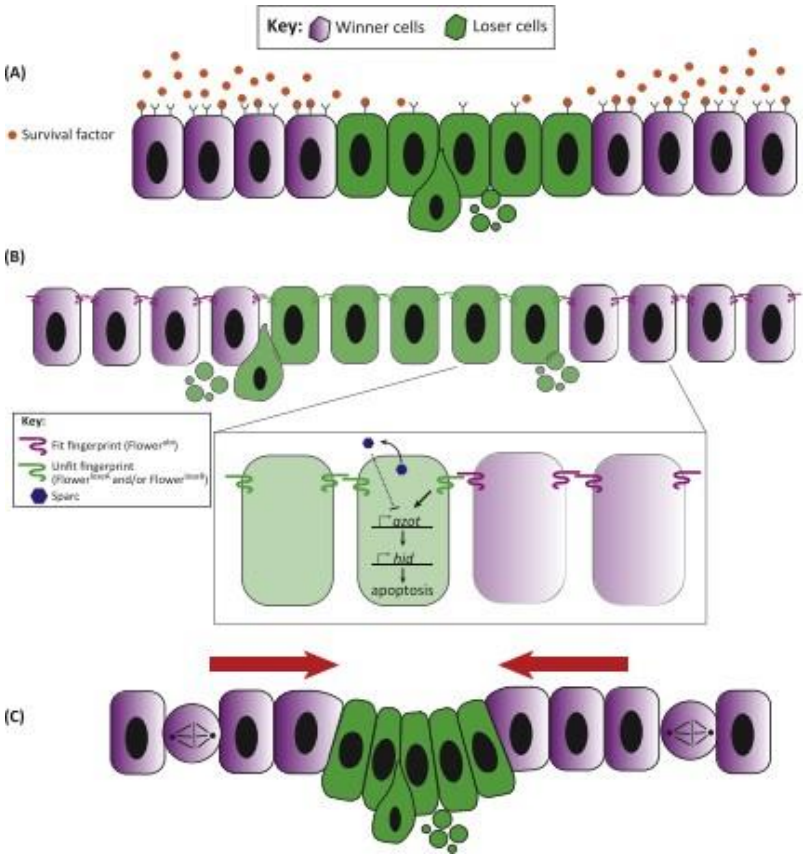

Figure 1.2 – Types of cell competition. (A) – Competition for survival factors. (B) – Competition through fitness comparison. (C) – Competition through mechanical forces. B is the only type of cell competition that requires direct cell-cell contact. Adapted from (Merino et al., 2016).

1.1.2 – The Flower code

The *flower (fwe)* gene, previously mentioned as having an essential role in cell competition through fitness comparison, was first identified in a supercompetition assay. This assay was performed in the wing imaginal disc of *Drosophila* with the aim of unravelling early upregulated genes in cell competition. *fwe* was found to be upregulated in the loser cells and it is proposed to code for a calcium channel with three transmembrane domains. This gene was showed to be conserved and can produce different isoforms of the same protein, due to alternative splicing (Rhiner et al., 2010). In *Drosophila*, the *fwe* locus gives rise to three different isoforms: fwe^{ubi}, fwe^{loseA} and fwe^{loseB} (Figure 1.3). These three isoforms

differ solely in the extracellular C-terminal domain. The name *fwe*^{ubi} was given because this isoform is ubiquitously expressed in imaginal discs. As for *fwe*^{loseA} and *fwe*^{loseB}, they were found to be expressed only in loser cells and are required for loser cell elimination (Rhiner et al., 2010).

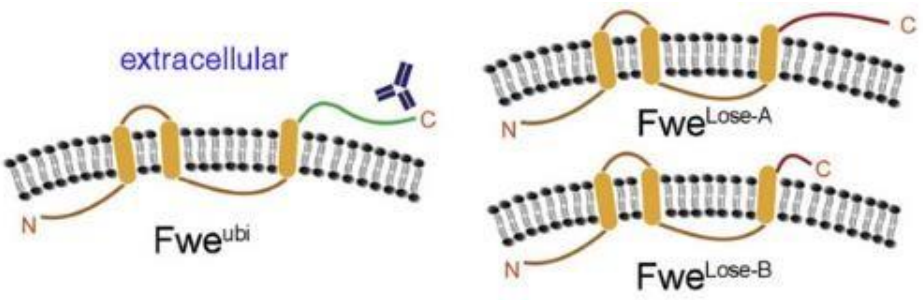

Figure 1.3 – Schematic of the three flower isoforms found in Drosophila, which only differ in the C-terminal domain. fwe^{ubi} *is ubiquitously expressed, while the expression fwe*^{loseA} *or fwe*^{loseB} *is sufficient to mark cells as losers. Adapted from (Rhiner et al., 2010).*

Whenever a cell becomes unfit, it will express, and expose to the extracellular matrix, a *fwe*^{lose} isoform which is recognized by the adjacent winner cell, expressing *fwe*^{ubi}. In this so-called heterotypic environment, cell competition occurs to eliminate unfit cells. However, when loser cells communicate among them without winner cells in the vicinity, or vice-versa, cell competition is not triggered, leading to the accumulation of populations of unfit cells (Figure 1.4) (Rhiner et al., 2010).

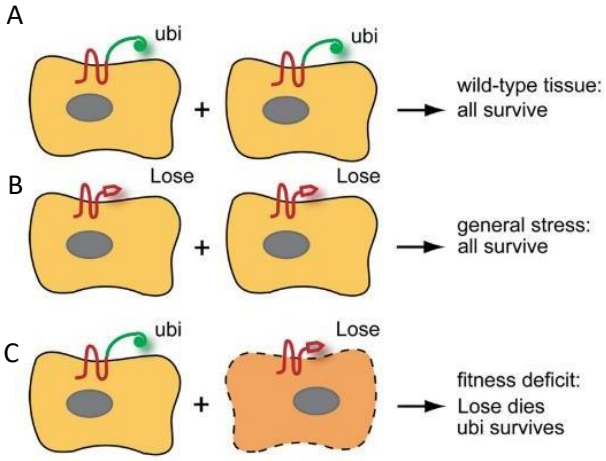

Figure 1.4 – Model representing different scenarios of cell-cell communication using fwe isoforms. (A) – When two winner cells interact, both of them survive, since cell competition is not triggered. (B) – When two loser cells interact, none of them dies, because, once again, there is an absence of cell competition. (C) – When a winner cell recognizes a loser cell, due to its fitness deficit, cell competition is triggered, and the loser cell enters in apoptosis. Adapted from (Rhiner et al., 2010).

1.1.2.1 - Fwe code differences in epithelial cells and neuronal tissues

Nonetheless, the role of the different isoforms as well as the fate of the loser cells are not as straightforward as it seems. Nowadays, there is evidences pointing to the fact that the expression of different *fwe*^{lose} isoforms does not necessarily imply the induction of apoptosis of loser cells. A good example of that are the experiments performed in *Drosophila* retina, where *fwe*^{loseB} is the only lose isoform and promotes the culling of extra non-functional ommatidia generated during the retina formation.

Additionally, an important molecule was found to be expressed in the loser cells as its defensive mechanism, preventing these cells from being eliminated by apoptosis. This molecule is called Secreted Protein Acidic and Rich in Cysteine (SPARC) and it was found to be early upregulated in loser cells during cell competition. SPARC is a calcium binding glycoprotein which promotes the survival of the loser cells in situations of cellular stress. SPARC has not been directly associated with *fwe* pathway and therefore it is postulated that the expression of SPARC may constitute a general stress response of the loser cells and may prevent inappropriate elimination of cells experiencing a transient fitness deficit. SPARC expression can be induced tissue injury, morphogenesis or tissue remodelling (Clavería and Torres, 2016; Portela et al., 2010).

To conclude, there are three main fitness levels that need to be integrated for a cell to be labelled as "loser": (1) – presence of a fwe^{lose} isoform; (2) – level of SPARC expression and (3) – the level of lose isoforms in the neighbouring cells (each cell compare the levels of fwe^{loseA} *and* fwe^{loseB} with the vicinity, and cells that express more fwe^{lose} isoform are killed) (Merino et al., 2015, 2016).

1.1.2.2 - An example of the different roles of fwe^{lose} isoforms: neuronal culling

Drosophila eye is composed by approximately 800 ommatidia, each of which is formed by eight specialized and different photoreceptors, four cone cells, and pigments cells (Merino et al., 2013). During the eye development, some incomplete ommatidia are formed at the periphery of the retina and they must be eliminated at the pupal stage. The process of purging unwanted neurons from the periphery of the retina is known as neuronal culling (Merino et al., 2015) and requires the involvement of the *fwe* code (Merino et al., 2013). In fact, it was shown that fwe^{loseB} expression is restricted and required for the elimination of the peripheral ommatidia, while fwe^{ubi} and fwe^{loseA} are broadly expressed across the retina (Figure 1.5).

The neuronal culling occurs 40-46h after pupae formation (APF) and the expression of fwe^{loseB} in the neurons in the edge of the retina is activated 36h-44h APF. Therefore, there is a specific timepoint where the neuronal culling and the expression of fwe^{loseB} coincide (40h-44h APF) (Merino etal., 2013). During this time window, *fwe*-dependent cell death is maximum (Figure 1.5)

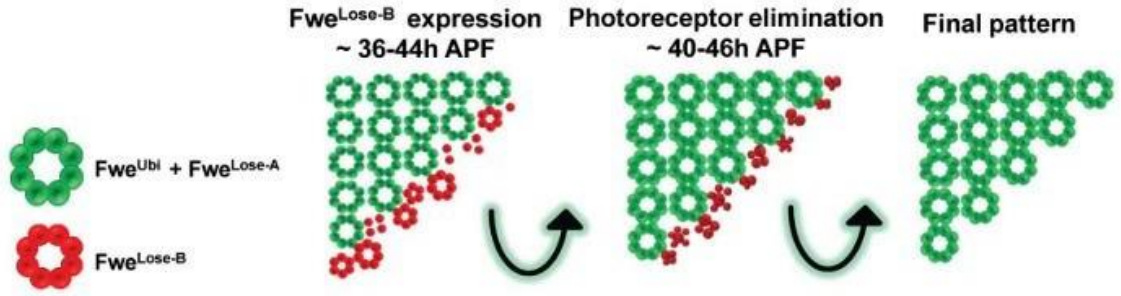

Figure 1.5 - Scheme depicting the role of fwe isoforms in neuronal cell death at the pupal retina stage. fwe^{ubi} and fwe^{loseA} are ubiquitously expressed in the retina. During pupal retina development, between 36 and 44 hr after pupae formation (APF), locally restricted expression of fwe^{loseB} is induced in neuronal cells of incomplete ommatidia units that are going to be eliminated and is sufficient and necessary to cull unwanted neurons. Adapted from (Merino et al., 2013).

With these experiments, it becomes clear that the expression of the *fwe* code is tissue specific (Merino et al., 2013; Moreno et al., 2015).

1.1.3 – Processes downstream of Fwe

After the fitness comparison phase, the information is transduced and integrated. One of the key proteins involved in the integration of the signal is Azot. *azot* gene is composed by only one exon encoding a cytoplasmic protein with four calcium binding EF-hand domains. This gene, found to be upregulated in loser cells during the cell competition process, acts as a cell-fitness checkpoint essential to decide if the cell undergoes apoptosis or not (Merino et al., 2015). When *azot* is expressed, it will activate the expression of the pro-apoptotic gene *hid*, which in turn triggers apoptosis of the loser cells and induces its clearance from the tissue (Figure 1.2 B) (Merino et al., 2016). Interestingly, in a context where *azot* is depleted (*azot* knockout) loser cells become abundant in tissues, leading to morphological aberrations, and tissue degeneration. On the other hand, an extra copy of *azot* leads to an increase in tissue health and prolongs flies' lifespan (Merino et al., 2015).

Taken all the information together, it is concluded that the accumulation of mutations is not enough to dictate the fate of a cell. It is the balance between the expression levels of different genes (mainly *fwe*, *azot* and *SPARC*) and the ration winner/loser cells that ensures the final decision of cell elimination, in the specific case of cell competition by fitness comparison.

1.1.4 – *fu2*

The supercompetition assay performed by Rhiner et al. in 2010 allowed the identification of different genes early upregulated in loser cells, through an expression microarray. This microarray was performed using the mRNA of cells in the wing imaginal disc that were under a supercompetition process. Supercompetition was induced by the generation of clones of loser GFP-positive cells (expressing basal levels of *dMyc*) surrounded by supercompetitor cells (overexpressing *dMyc*) (Figure 1.6).

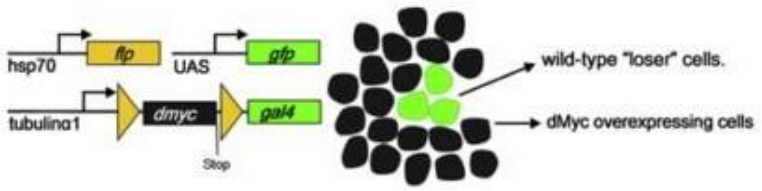

Figure 1.6 – Schematic of the strategy used to induce supercompetition. A short heat-shock activates de expression of flipase (flp) enzyme in a random subset of cells. This enzyme will act on FRT sequences (yellow triangles), promoting the excision of dMyc and stop sequence, which allows the expression of gal4. When Gal4 is expressed, it will bind to the UAS sequence, activating the expression of GFP. Therefore, cells expressing GFP are loser cells, since the dMyc expression levels are basal. In cells where flp was not active, dMyc will not be excised (it will be expressed instead), increasing the levels of dMyc and turning these cells into supercompetitors. Adapted from (Rhiner et al., 2010)

Early upregulated genes are interesting to be analysed, since they might play an initiating role in cell competition. The early upregulated genes identified were then confirmed by mRNA fluorescence *in situ*

hybridization (FISH). Among the genes that were differentially expressed during cell competition was *fwe* (previously described) and *fu2*, a transcriptional factor with nine predicted zinc finger domains and one zinc-finger associated (ZAD) domain, found to be expressed as early as 12h-24h after clone induction (Rhiner et al., 2010). *fu2* gene is composed by two exons and it has two annotated transcripts.

Although *fu2* function is not clear, the biochemical structure of the protein may give some clues about its biological function. Zinc finger domains are one of the main structures involved in eukaryotic protein-nucleic acid interaction (Doublie and Tabor, 1998). Zinc finger domains were first discovered in the transcription factor IIIA (TFIIIA), found in *Xenopus*. Further studies proved that zinc finger domains are present in proteins that intervene in *Drosophila* segmentation, such as *Kruppel* or *Hunchback*, or in regulatory proteins of lower eukaryotic organisms (Doublie and Tabor, 1998). Zinc finger can be defined as a small, functional and independently folded domain that requires the interaction of one or more zinc ions to stabilize the structure (Laity et al., 2001). Approximately 80% of *Fu2* structure is composed by zinc finger domains, suggesting that this protein may bind to the DNA.

Recently, a study reported that *fu2* and *fwe* are genetically related, which suggests that *fu2* is involved in cell competition events. Additionally, the absence of *fu2* seems to give a stronger phenotype in the imaginal discs of *Drosophila* (particularly in the eye-antenna disc), giving rise to malformations of the cone cells. Thus, an initial analysis of the imaginal discs should be performed in a context of cell competition.

1.2 – *Drosophila melanogaster* as biological model

Drosophila melanogaster, also known as fruit fly, is a small insect belonging to the *Diptera* order and *Drosophilidae* family (Hales et al., 2015). Over the past four decades, *Drosophila melanogaster* has become a predominant model used in science research and to study human diseases (Jennings, 2011).

Thomas Hunt Morgan, considered the “father” of *Drosophila* research, is responsible for refining the theory of gene inheritance, firstly established by Gregor Mendel, long before it was even established that DNA is the genetic material (Jennings, 2011)

1.2.1 – Advantages of the *Drosophila* model in science

Nowadays, fly genetics are systematically applied to the study of development, physiology and behaviour. It allows for the understanding of cell biology, basic genetic and molecular mechanisms, with many being conserved among higher animals and humans. There are several factors turning *Drosophila* into a powerful model in science. They are easy and cheap to maintain, with a short life cycle that allows for the rapid generation of large numbers of progeny. Moreover, *Drosophila* has a simple genome composed by 4 pairs of chromosomes and every gene may be targeted for genetic manipulations including orthologous genes associated with human diseases, such as Alzheimer’s disease (Roote and

Prokop, 2013). The lack of redundancy among genes turns *Drosophila* into a great a biological model for loss-of-function screenings.

1.2.2 – *Drosophila* life cycle

Concerning *Drosophila* life cycle, they undergo a four-stage life cycle; egg, larva, pupa, and adult fly (Figure 1.7). At 25°C, embryonic development lasts approximately 21 hours (Roote and Prokop, 2013). The hatched larvae molt twice and throughout the molting process, since the start until the end of the molting, larvae are known as instar. Therefore, *Drosophila* has three instar phases: 1st instar take 2 days to molt into 2nd then 3rd instar larvae. The cuticle of the third instar larvae is harder and will eventually give rise to the puparium (Flagg, 1979) (outer case of the pupa). Pupal initial stage (0-1 hour APF) shows a whitish cuticle and the cuticle darkens during pupa maturation. Hatched flies become mature adults and remain fertile during all their life (Flagg, 1979).

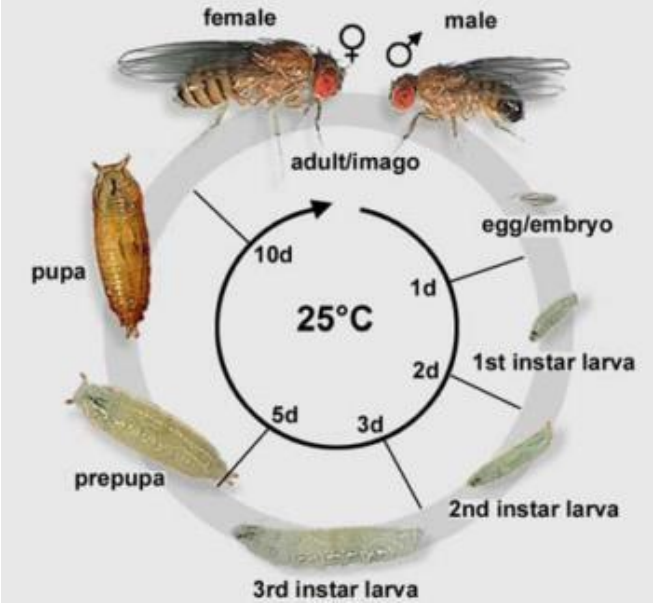

Figure 1.7 - Drosophila four stage life cycle. 21 hours after egg laying the larvae hatches. After 5 days larvae reach pupation stage. 10 days after egg laying a new fly is born. Adapted from (Roote and Prokop, 2013)

All larvae that suffers metamorphosis have small epithelial structures called imaginal discs. There is a total of 19 imaginal discs in the whole *Drosophila* larvae, including wing, eye-antennal and leg discs (Aldaz and Escudero, 2010). *Drosophila* has two eye-antennal imaginal discs, each of which composed by two cellular layers: the main epithelium (ME) and the peripodial epithelium (PE). ME is formed by columnar cells, while PE is formed by squamous cells (Haynie and Bryant, 1986). It is the ME of the eye imaginal disc that will give rise to the retina, among other structures. The differentiation of the eye disc progresses in a posterior-to-anterior direction due to a wave of differentiation called morphogenetic furrow. This wave is responsible to differentiate cells from the eye discs into retinal cells (Ready et al., 1976; Tomlinson and Ready, 1987). The localization of the eye imaginal discs in the larvae and their morphology are represented in Figure 1.8.

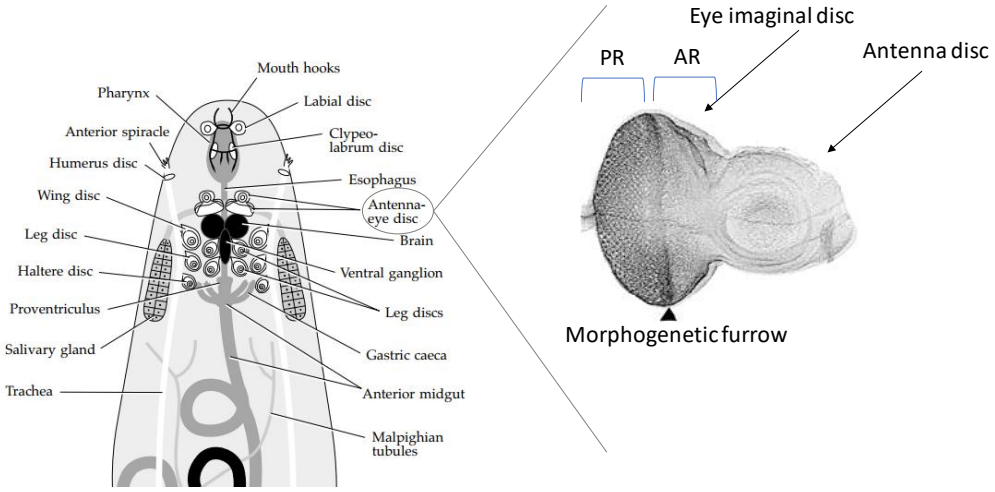

Figure 1.8 - Scheme showing the localization of the eye imaginal discs in Drosophila larvae (left). Detail of the morphology of the eye-antenna disc. In the eye disc portion, the differentiated cells are distinguished from the undifferentiated ones, through the morphogenetic furrow, which swipes the eye discs from the posterior region (PR) to the anterior region of the disc (AR), close to the antenna disc. Adapted from Tyler, 2000 and Singh and Kango-Singh, 2013.

1.2.3 – *Drosophila* as a model to study Alzheimer's disease

The fact that the genes and the cellular mechanisms of *Drosophila* is conserved turns it into an ideal model organism to study human diseases, such as Alzheimer's disease. In fact, approximately 70% of disease-associated human genes have a functional orthologue in *Drosophila*. Moreover, there is a considerable similarity between the central nervous system of flies and humans, in terms of cells types (neurons and glia) and the neurotransmitters, which explains why flies are commonly used to study neurodegenerative diseases (Lenz et al., 2013).

Alzheimer's disease is considered the most prevalent neurodegenerative disease among the elderly, affecting more than 24 million people in the world. This disease is characterized by neuronal cell loss and by the accumulation of two specific proteins: amyloid plaques enriched in the amyloid-β (Aβ) peptide and neurofibrillary tangles enriched in hyperphosphorylated Tau. Both proteins (Aβ and Tau) tend to form toxic aggregates (Fernandez-Funez et al., 2015). Aβ is produced by proteolytic processing of the amyloid precursor protein (APP). APP processing happens by one of two pathways: the non-amyloidogenic pathway or the amyloidogenic pathway. When APP processing follows the amyloidogenic pathway, two small peptides, among other peptides, known as $A\beta_{40}$ and $A\beta_{42}$ are secreted to the extracellular matrix (Mhatre et al., 2014). $A\beta_{42}$ is considered the predominant amyloidogenic peptide, since it forms insoluble extracellular aggregates more easily. Additionally, previous studies showed that the expression of $A\beta_{42}$ causes phenotypes in flies. When this peptide is overexpressed in the eye of the flies, it produces a rough eye texture as well as blindness (Prüßing et al., 2013). Since $A\beta_{42}$ induces such a strong phenotype in the eye of the flies, the overexpression of this protein is often stimulated in the developing eye, including the eye imaginal discs. Previous studies report the generation of a model system in *Drosophila* eye where the overexpression of $A\beta_{42}$ is induced in the differentiated neurons, using the Glass Multiple Repeat promoter (GMR) – GMR-Gal4 > *UAS*- $A\beta_{42}$. The penetrance of the phenotype generated by this construct is 100%, turning it into a reliable tool to study neurodegeneration (Cutler et al., 2015).

1.2.4 – Genetic tools in *Drosophila*

As previously mentioned, one of the greatest advantages of *Drosophila* is the ease to manipulate them genetically, thus creating transgenic flies. There are different classes of transgenic flies, including flies carrying reporter genes (e.g. *GFP* or *mCherry*) or the *UAS*/Gal4 system, for example. Reporter genes are essential for all *Drosophila* researchers, allowing, among other aspects, the analysis of promoters and gene expression patterns or the discovery of new interactions between proteins (Naylor, 1999). The *UAS*/Gal4 system, is a binary system which relies in: (1) Gal4, a transcriptional activator from yeast, responsible for galactose metabolism, that may be expressed in a tissue-specific manner. This specificity is given by the promoter used to drive *gal4* expression. (2) Upstream Activation Sequence (*UAS*) - the target DNA sequence of Gal4 (Elliott and Brand, 2008). When crossing flies expressing *gal4* with *UAS* lines the sequences downstream of *UAS* are activated (Roote and Prokop, 2013) (Figure 1.9).

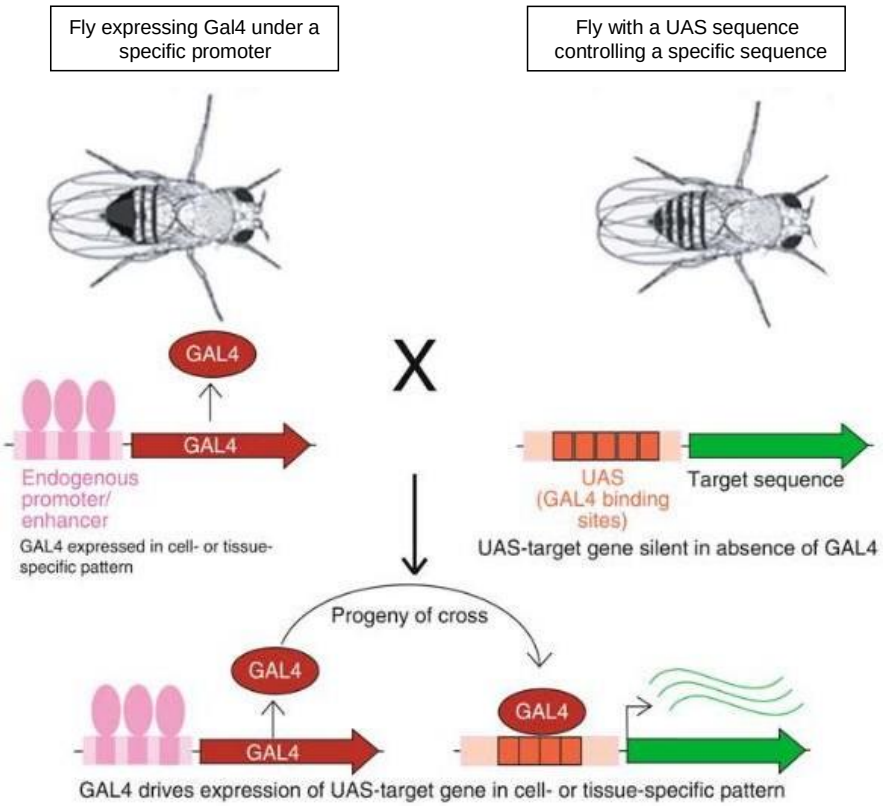

Figure 1.9 – Schematic of UAS-Gal4 system. When flies expressing gal4, are crossed with flies containing a UAS sequence, there will be expression of the sequence downstream of UAS in the progeny. In the absence of Gal4, the sequence downstream of UAS is silent. Adapted from (Elliott and Brand, 2008)

A key factor of this system is the spatial-temporal feature, achieved by combining gal4 gene with different types of promoters (e. g. Hsp70-Gal4 allows the expression of Gal4 upon heat-shock treatment; glass multiple reporter (GMR)-Gal4 drives the expression of the UAS-associated gene of interest in the neurons) (Elliott and Brand, 2008; Tettweiler and Lasko, 2007).

Transgenic flies can be generated by different molecular tools. The classical method, and most used so far, is based on the use of transposable elements. Transposable elements are DNA fragments that are inserted in the genome upon DNA replication and can be maintained over many generations. With these elements, it is possible to tag genes, induce mutations or insert sequences (such as *gal4* sequence) in the genomic DNA (gDNA) of multiple organisms (Tettweiler and Lasko, 2007). In *Drosophila,* the most used transposable element is the P-element (Bachmann and Knust, 2008).

However, new genome engineering technologies based on the induction of double strand breaks (DSB) have been increasingly used. The most recent genome engineering technology is called Clustered Regularly Interspaced Short Palindromic Repeats-CRISPR associated protein 9 (CRISPR-Cas9) system.

CRISPR-Cas9, first discovered in *Escherichia coli* in 1987, is naturally found in a large number of prokaryotic species and is used to specifically recognize and eliminate foreign DNA, such as phage genomes. In 2007, the hypothesis that CRISPR-Cas9 could act as an adaptative immune system was experimentally proved, using *Streptococcus thermophilus* as biological model (Bondy-Denomy and Davidson, 2014; de la Fuente-Núñez and Lu, 2017). In these bacteria, fragments from an invading foreign DNA can be recognized and inserted into a specific region of the genome, creating the CRISPR locus. The fragments inserted in the locus are called protospacers. In response to viral or phage infections, CRISPR locus is transcribed and processed in a matured CRISPR RNA (crRNA), containing the protospacer sequences. crRNA is responsible to direct Cas enzymes to the target genomic region (Figure 1.10). Cas enzymes are endonucleases with the ability to induce DSB in a specific target DNA site (Zhang et al., 2016).

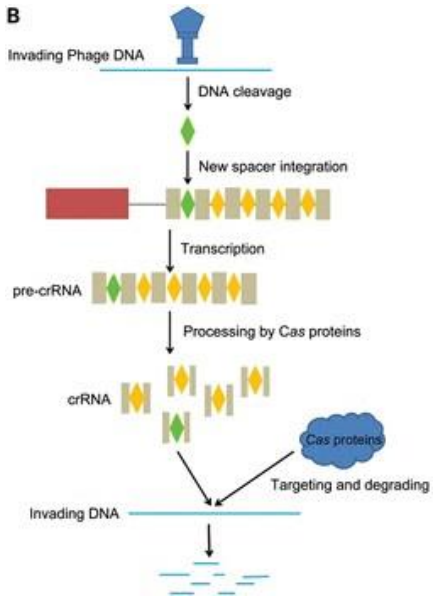

Figure 1.10 – Schematic showing how CRISPR-Cas system works in Escherichia coli. When exogenous DNA is injected into the bacteria, DNA is cleaved and integrated in CRISPR locus. Then, upon a second infection, CRSIRP locus is transcribed and processed into discrete crRNA units. Each unit contains one protospacer that will guide one Cas protein to a specific target site and induce a DSB. Adapted from (Zhang et al., 2016)

To date, three different CRISPR-Cas systems are known, based on the structure of Cas proteins and on the number of molecules required for Cas to cut the DNA. CRISPR-Cas type I and III only require crRNA for targeting Cas, while CRISPR-Cas type II, also requires a trans-activating crRNA (tracrRNA). Moreover, Type I and III systems rely on Cas nucleases comprised by multiple subunits, while type II system requires only a single polypeptide: Cas9 (Sternberg and Doudna, 2015). In type II CRISPR systems, crRNA interacts with tracrRNA, giving rise to a small guide RNA (sgRNA), that directs the Cas9 enzyme to a specific DNA sequence (complementary to the protospacer) (Ma et al., 2014). When Cas9 reaches the target site, usually with 20 base pairs (bp) length and immediately followed by an NGG motif, called protospacer domain (PAM), it cleaves both strands of the DNA target precisely 3 nucleotides upstream PAM (Ma et al., 2014). Protospacers present in the CRISPR locus are not cleaved due to the absence of PAM sequences (Sander and Joung, 2014).

Type II CRISPR-Cas is the only system that has been used for genome editing, due to its simplicity and efficiency (de la Fuente-Núñez and Lu, 2017). To use this system, only two components are required: a functional Cas9 nuclease and a sgRNA. 20 nucleotides in the 5' end of this sgRNA are responsible to direct Cas9 to the target site, using standard RNA-DNA complementarity. These 20 nucleotides must recognize a sequence immediately upstream of the PAM sequence (Figure 1.11). This way, it is possible to direct Cas9 to any DNA target region, by simply altering the first 20 nucleotides of the 5' of the sgRNA (Sander and Joung, 2014).

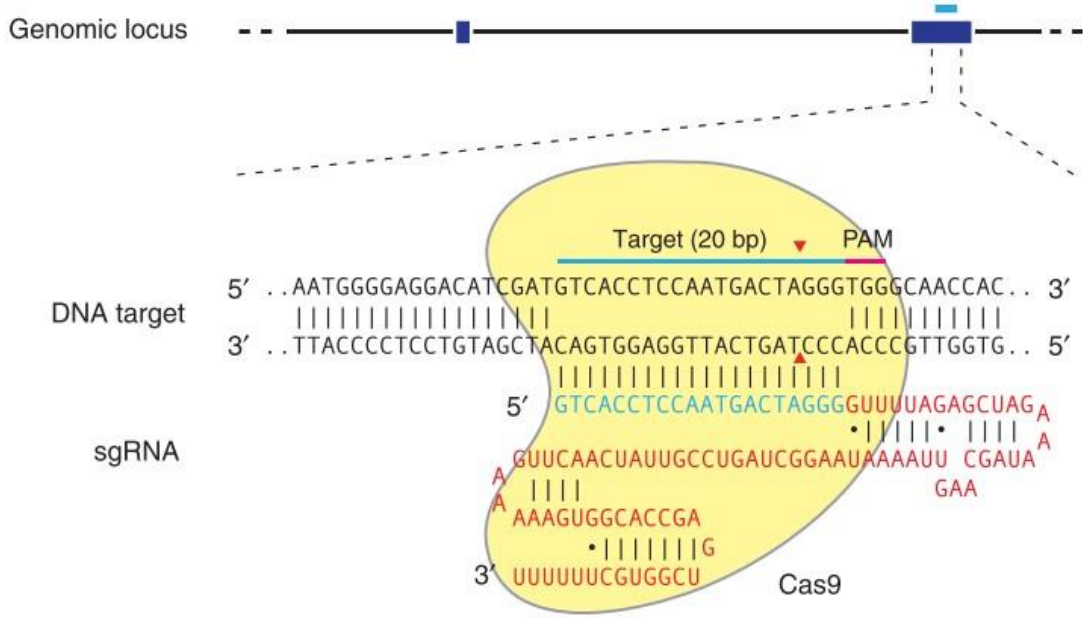

Figure 1.11 - Schematic of Cas9 guided by an sgRNA. The sgRNA is composed by two fused RNA molecules (the crRNA and the tracrRNA). The recognition of the gDNA by the sgRNA occurs through the presence of 20 nucleotides at the 5' end of the sgRNA (blue region) complementary to the target region. In the gDNA, the target region must be immediately followed by a PAM sequence. Note that the cut performed by Cas9 enzyme (yellow shape) occurs 3 nucleotides upstream PAM sequence (red arrowhead). Adapted from (Ran et al., 2013).

Since the discovery that CRISPR-Cas9 can be used for genome editing, new applications of this system had been emerging, such as generation of mutants (e.g. knockout / knock-in generation), identification of gene pathways or execution of high-throughput genetic screens (de la Fuente-Núñez and Lu, 2017). Knockout (KO) mutation allows the performance of reverse genetics, leading to the identification of gene functions. The basic step to induce a KO mutant is to create a DSB. This cut will be repaired by one of two well-known DNA repair pathways: nonhomologous end joining (NHEJ) or homology directed repair (HDR). When NHEJ is induced, broken ends of the DNA are re-joined without regard for homology and often creating insertion/deletion (indels) mutations are generated, which can disrupt the expression of a gene, since both ends of the break are ligated (Carroll, 2014). This mechanism restores the chromosome continuity and prevents chromosomal translocation events. Whenever a "repair template" is delivered to the cell, HDR-mediated repair can be induced to delete a target gene and, at the same time, introduce the "repair template" into the cells' gDNA (Figure 1.12) (Newman et al., 2015; Sander and Joung, 2014).

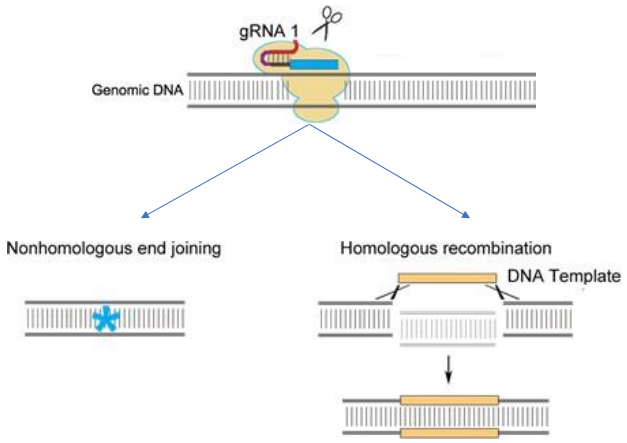

Figure 1.12 - Schematic of DNA break repair. When Cas9 induces the DSB, DNA can be repaired through one of two mechanisms: Nonhomologous end joining or by Homologous recombination. The last mechanism requires the delivery of one "repair DNA template", leading to the insertion of an exogenous sequence into the gDNA of the organism. Adapted from flycrispr website (http://flycrispr.molbio.wisc.edu/)

The efficiency of HDR was already proved to be higher when is preceded by a DSB in the gDNA (Gaj et al., 2013). Therefore, currently "repair templates" are designed to insert specific sequences into the gDNA of different organisms, including *Drosophila*, upon the induction of one or more DSB. One key factor is the creation of homology arms, homologous to the regions adjacent to the cut(s) site(s), flanking the insertion region (Baena-Lopez et al., 2013). The "repair template", as well as the sgRNA(s), is introduced in a targeting vector, which is then injected in *Drosophila* embryos (Baena-Lopez et al., 2013). As for the delivery of Cas9, there are several approaches, including viral transfection, delivery through plasmid (to generate stable lines expressing Cas9) and direct injections of the protein (LaFountaine et al., 2015; Luther et al., 2018). A very common strategy in *Drosophila* is the use of fly lines expressing Cas9 endogenously. More recently, germline specific promoters, such as nanos (nos) or vasa promoters, have been increasingly used due to the high efficiency of mutagenesis when Cas9 is exclusively expressed in the germline (Baena-Lopez et al., 2013).

CRISPR/Cas9 technology brought many advantages over molecular biology techniques, namely, easiness of execution, low cost and it allows the induction of one or multiple mutations, by using multiple sgRNAs at once. However, there are also some limitations, such as the off-target effects (mutations in unspecific regions), generation of different mutant alleles or a strict dependence of a PAM sequence (Ribeiro et al., 2018). For these reasons, optimization of CRISPR/Cas9 is still required for all the animal models.

1.3 – Goal of the project

It is known that *fu2* is expressed specifically in loser cells, in a supercompetition context. However, it is not known if it is strictly required for loser cell death and/or if it can act in other cell competition contexts. Thus, the goal of this project is to unravel if *fu2* is required for loser cell elimination, using different cell competition contexts, such as in neurodegenerative disease (Alzheimer's disease) and during neuronal culling.

2 – Materials and Methods

2.1 – Molecular Biology Techniques

Drosophila genomic DNA extraction

For each genomic DNA (gDNA) extracted from a single fly, Squishing Buffer 1X (200mM Tris-HCl pH8, 20mM EDTA, 500mM NaCl) and Proteinase K (NZYTech #MB01901) (20mg/mL) were used in a final volume of 50µL. Flies were squished using a pipette tip and incubated at 37ºC for 30 minutes to maximize the activity of the enzyme. To inactivate the enzyme, samples were incubated at 95ºC for 3 minutes.

DNA quantification

DNA concentration was measured using Nanodrop spectrophotometer (ThermoFisher).

Sequencing procedure

The sequencing reactions were performed according to STABVIDA's instructions, with 10µL of DNA and 3µL of sequencing primer (10µM), in a final volume of 13µL. DNA concentration equal or superior to 20ng/µL or 100ng/µL for PCR products and plasmids, respectively, was used. Primers used to sequence the fragments are listed in Table 2.1.

Fragments were sequenced at STABVIDA's facilities using the Sanger method and the sequencing results were analysed with SnapGene editor software, by comparing the reads with the expected DNA template.

Table 2.1 - Primers used for sequencing reactions. The column in the middle shows the sequence of each primer (from 5' to 3') and the rightmost column shows the target of each set of primers. Each sequencing reaction contained only one primer.

Primer Name	Primer Sequence	Target region
U63seqfwd	ACGTTTTATAACTTATGCCCCTAAG	Region of pCFD5 containing sgRNAs
pCFD5seqrev	GCACAATTGTCTAGAATGCATAC	
pBH111	CTCACTGCAATTAAGCAATAACCG	*fu2* 5'HA
Fu2exon1 16Rv	GTGCTCACATCCTGATCCTG	
pFu2_490Fw	CCATCAGTTGCAGCACAAGATGG	*fu2* 3'HA
pBH112	GATTTCGAGGCGATCAAGATCCG	
M13 Fw	GTAAAACGACGGCCAGT	pCR™-Blunt II-TOPO™+ 5'HA and pCR™-Blunt II-TOPO™+3'HÁ
M13 Rv	CAGGAAACAGCTATGAC	
pBH111	CTCACTGCAATTAAGCAATAACCG	*fu2* locus
Fu2 3HA Rv	GGATTCTATGTTGACCTGAACG	

DNA amplification

All the DNA used for different applications was amplified using 3-step Polymerase Chain Reaction (PCR) protocols. Two different DNA polymerases were used: Platinum SuperFi DNA Polymerase (ThermoFisher #12351010), for DNA used for cloning and/or sequencing, and DreamTaq DNA polymerase (Invitrogen #EP1712), for genotyping. Reactions were performed according to the manufacturer's conditions. The annealing temperatures (Ta) differ according to the set of primers and the type of DNA polymerase used.

Regarding Platinum SuperFi DNA Polymerase (ThermoFisher # 12351010), reactions were cycled in BIORAD T100 Thermal Cycler, using the following PCR program: (98ºC 3 min, 35 cycles of [98ºC 10 s, Ta 10 s, 72ºC 30s/kb], 72ºC 5 min, 4ºC hold).

With respect to DreamTaq DNA polymerase, DreamTaq Green Master Mix 2x (Thermo Scientific #K1081) was used. Samples were cycled in BIORAD T100 Thermal Cycler, following Touchdown protocol (Korbie and Mattick, 2008), optimized for DreamTaq. The following program was used (94ºC 30 sec, 5 cycles of [94ºC 15 s, Ta+3ºC 30 s, 70ºC 3 min], 5 cycles of [94ºC 15 s, Ta 30 s, 70ºC 3 min], 40 cycles [94ºC 15 s, Ta-3ºC 30 s, 70ºC 3 min], 70ºC 6 min, 4ºC hold).

Table 2.2 contains all set of primers used for PCR, along with the Ta and the length of each amplified DNA fragment. Ta values were calculated using ThermoFisher Tm calculator (ThermoFisher). Template DNA was used in a final concentration of ~100 ng/ µL, when using DreamTaq DNA polymerase, and ~200ng/ µL, when using Platinum SuperFi DNA Polymerase.

Set of primers U63seqfwd and pCFD5seqrev were used to perform a colony PCR experiment. This reaction helps to determine the presence of an insert DNA in plasmids. It is performed as a normal PCR, however one bacterial colony is used as "DNA template", instead of extracted DNA.

*Table 2.2 - Set of primers used for DNA amplification and respective annealing temperature (Ta). The table shows the primer sequence (from 5' to 3'), the annealing temperature used for each set of primers, the length of the amplified fragment and the type DNA polymerase used for each PCR experiment. Regions in **bold** represent the gRNA sequence. Regions underlined represent cut sites for each enzyme. *A gradient of temperatures was used to determine the optimal annealing temperature.*

Set of primers	Primer Name	Primer Sequence	Amplified fragment length	Ta (ºC)	DNA polymerase
1	pBH111	CTCACTGCAATTAAGCAATAACCG	826bp	63.2*	Platinum SuperFi
	Fu2exon1 16Rv	GTGCTCACATCCTGATCCTG			
2	pFu2_490Fw	CCATCAGTTGCAGCACAAGATGG	742bp for WT 838 bp for fu2::3xHA-tag	66.2*	Platinum SuperFi
	pBH112	GATTTCGAGGCGATCAAGATCCG			
3	Fu2 sgRNA -95 Fwd	GCGGCCCGGGTTCGATTCCCGGCCGATGC**AAATAAAACGCGTTGGTCAATGG**GTTTTAGAGCTAGAAATAGCAAG	247bp	61ºC and increases 0,5ºC per cycle until a temperature of 72ºC is reached	Platinum SuperFi
	Fu2 sgRNA -8 Rev	ATTTTAACTTGCTATTTCTAGCTCTAAAAC**CGGGACGAGTCTCGCTGTAG**TGCACCAGCCGGGAATCGAACCC			
4	NotI-5'sgRNA-5'HA Fw	CGGCGGCCGCCCATTGACCAACGCGTTTTATTTGGACGGGAATAACACACTAACCGCATGG	1090bp	70.1*	Platinum SuperFi
	NdeI-5'HA Rv	CGCATATGCAATGTCCAATCTACCACGATAGTATCGATATGTCG			
5	SpeI-3'HA Fw	CGACTAGTCCGAGAAATAGAACAACATATTTACATGTTTAATAAGCTTAGTTGATAGGTCGG	1065bp	72*	Platinum SuperFi
	BglII-3'HA-3'sgRNA Rev	CCAGATCTCTACAGCGAGACTCGTCCCGAGGGCTGCGCGGACCGCTGATCATG			
6	U63seqfwd	ACGTTTTATAACTTATGCCCCTAAG	834bp with gRNAs inserted 794bp for the empty vector	48.7	DreamTaq
	pCFDseqrev	GCACAATTGTCTAGAATGCATAC-			
7	pBH111	CTCACTGCAATTAAGCAATAACCG	2609 bp for WT 2098 bp for fu2 15.4 stock 300 bp for fu2 15.6	61.8 for Platinum 50.8 for DreamTaq	Platinum SuperFi or DreamTaq
	Fu2 3HA Rv	GGATTCTATGTTGACCTGAACG			
8	pFu2 upstream 5HA Fw	GCAATGTGGTCCAATCAGTTCATC	4229 bp for WT 3727 bp for 15.4 stock	52.4	DreamTaq
	pFu2 downstream 3HA Rv	GACTCGATGTCTGGCAACTG			

Samples analysis and DNA purification

PCR samples were loaded onto a 1% agarose gel in 1X TAE. DNA molecules were stained with GreenSafe Premium (NZYTech #MB13201). When performing PCR with Platinum SuperFi DNA polymerase, Gel Loading Dye, Purple (6X) (NEB), was used to increase the density and to keep track of the samples. Samples migrate to the anode when subjected to 80-100 volts. Gels were analysed in a transilluminator (BioRad). Molecular weight markers NZYDNA Ladder III (NZYTech #MB04401) or NZYDNA Ladder VI (NZYTech #MB08901) were used. DNA fragments were isolated from an agarose gel using a surgical blade and DNA were purified using Qiagen QIAquick Gel Extraction Kit.

Whenever the quantity of samples was large, iQIAxcel Advanced instrument (Qiagen) was used to run the samples, instead of a classical agarose gel. The samples were run on QIAxcel Advanced instrument (Qiagen) using the QIAxcel DNA Fast Analysis kit (Qiagen) and the 0M500 method (sample injection voltage of 5 kV and separation voltage of 5 kV) with a sample injection time of 15 s. During the run the QX DNA Size Marker was used (25–500 bp version 2.0), as was the corresponding QX Alignment Marker, 15/600 bp (Qiagen). QIAxcel ScreenGel software was used to analyse the results. Sample analysis was performed using a two-step approach. First, peaks were detected in the raw data. In a second step, the peak sizes and peak concentrations were determined by mapping the detected peaks against the reference size marker (Matsumoto et al., 2013).

Gibson Assembly

Gibson Assembly is a reaction that joins different overlapping DNA fragments in a single molecule. To do this, three enzymes are required: an exonuclease to create single-stranded 3’ overhangs; a DNA polymerase to fill in gaps generated upon annealed fragments; and a DNA ligase to seal the nicks. Figure 2.1 shows an example of two fragments being assembled through Gibson Assembly.

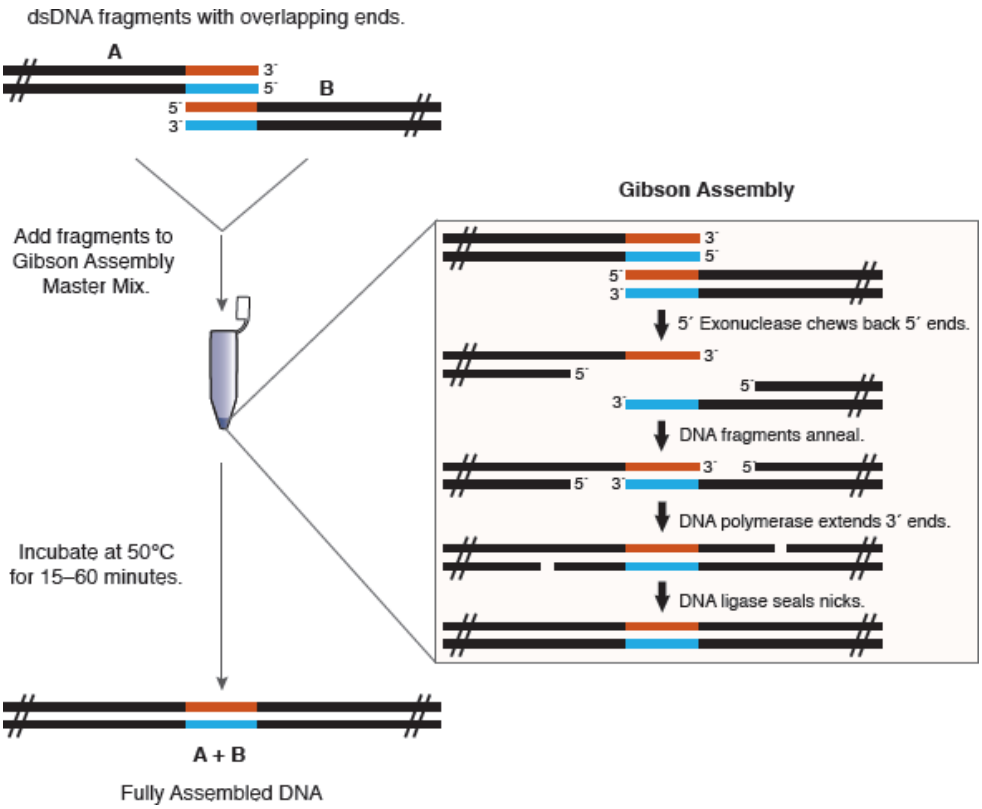

Figure 2.1 – Schematic of Gibson Assembly method. Different dsDNA fragments with overlapping regions are added to the Gibson Assembly Master Mix. The mix containing the DNA fragments is incubated at 50ºC for 60 minutes. The reaction comprises three steps: the generation of 3' overhangs by an exonuclease; the extension of the fragments by a DNA polymerase and the ligation of the fragments by a DNA ligase. The reaction's product consists in one single assembled DNA fragment. Adapted from Gibson Assembly® Master Mix Instruction Manual.

Gibson Assembly Reaction was performed using Gibson Assembly® Master Mix (NEB) and following the manufacturer's protocol, for a final volume of 20µL. The amount, in nanograms (ng), of fragment used for optimal assembly, was calculated through the formula given in Gibson Assembly® Master Mix Instruction Manual. 0,5 pmols of fragment was used.
The reaction was incubated at 50ºC for 1h.

Bacterial Transformation and Plasmid DNA extraction

Transformation is the process by which DNA is introduced into a host cell. The classical method of transformation consists on giving a heat shock (for 30 seconds at 37ºC), creating small pores or holes in the cell wall (Kilpatrick S.T., Krebs J. E., 2014).

Plasmid DNA was amplified by transformation into TOP10 chemically competent *Escherichia coli* (Invitrogen) cells. The transformants were selected on LB agar with either ampicillin (100 µg/µL) or kanamycin (50 µg/µL), depending on the original plasmid. Single cultures were isolated and cultured in 6 mL or 100 mL of LB medium for small or medium amounts of DNA required, respectively, with the appropriate antibiotic. Plasmid DNA was extracted either using QIAprep Spin Miniprep Kit (250) (QIAGEN) or Plasmid Midi Kit (25) (QIAGEN). Plasmid Midi Kit (25) (QIAGEN) was used to increase the amount of plasmid DNA needed for injection (1000ng/µL). DNA was quantified after extraction.

DNA ligation

DNA fragments were ligated using T4 DNA ligase (ThermoFisher #EL0011) following the manufacturer's conditions for a final volume of 20µL. The amount of each insert was calculated through the following formula assuming a 3 times excess of insert:
Ng of insert = [(ng of vector x Kb of insert)/Kb of vector] x 3/1
The ligation reaction was incubated at room temperature for 1h30 or overnight at 4ºC.

Restriction Digestion

DNA was digested using restriction enzymes and their respective buffer. The amount of DNA digested and final volume of digestion varied according to the needs of each fragment. The enzymes, and respective buffers, used for different ends are listed in Table 2.3. All DNA digestions were performed at 37ºC for 60-90 minutes.

Table 2.3- List of enzymes and their respective buffers.

Restriction Enzyme	Buffer
NotI-HF (NEB)	1X CutSmart®
NdeI (ThermoScientific)	1X Buffer O
SpeI-HF (NEB)	1X CutSmart®
BglII (ThermoScientific)	10x Buffer O
HindIII (ThermoScientific)	10x Buffer R
PstI (ThermoScientific)	10x Buffer O
SacII (NEB)	1X CutSmart®

2.2 – *fu*2 knockout generation

To create the KO lines, CRISPR/Cas9 system was used to induce DSB, flanking the coding sequence of *fu2.* Two sgRNAs were designed to target the 5' and the 3' end of the *fu2* gene. Two KO lines were generated by two different strategies.

In the first strategy, sgRNAs were cloned in separate vectors (pU6-BbsI-chiRNA, Addgene #45946). sgRNAs used (sgRNA 85/86 for the 5' end and sgRNA 87/88 for the 3' end) were generated before the beginning of this project. sgRNA 85/86 recognizes a region 578 bp upstream *fu2* transcription start site (TSS). sgRNA 87/88 recognizes a region 33 bp downstream *fu2* stop codon. sgRNA 85/86 and sgRNA 87/88 sequences are shown in section "6.1 – sgRNA sequences".

pU6-BbsI-chiRNA+sgRNA 85/86 (250ng/ µl) was co-injected with pU6-BbsI-chiRNA+sgRNA 87/88 (250ng/ µl) in *Drosophila* embryos expressing Cas9 under a germline specific promoter - nanos promoter (nos-Cas9 flies) (Bloomington 54591).

Single males from F0 generation (founder candidate flies) were crossed with a balancer fly stock[1] and the offspring was crossed again, separately, with balancer flies to establish each stock line. *fu2* KO candidate stocks were then genotyped (Figure 2.2). Note that no visible marker was used to identify KO flies. Therefore, a diagnostic PCR followed by sequencing procedures are mandatory. The KO stock with no sequencing errors was chosen to use in future experiments.

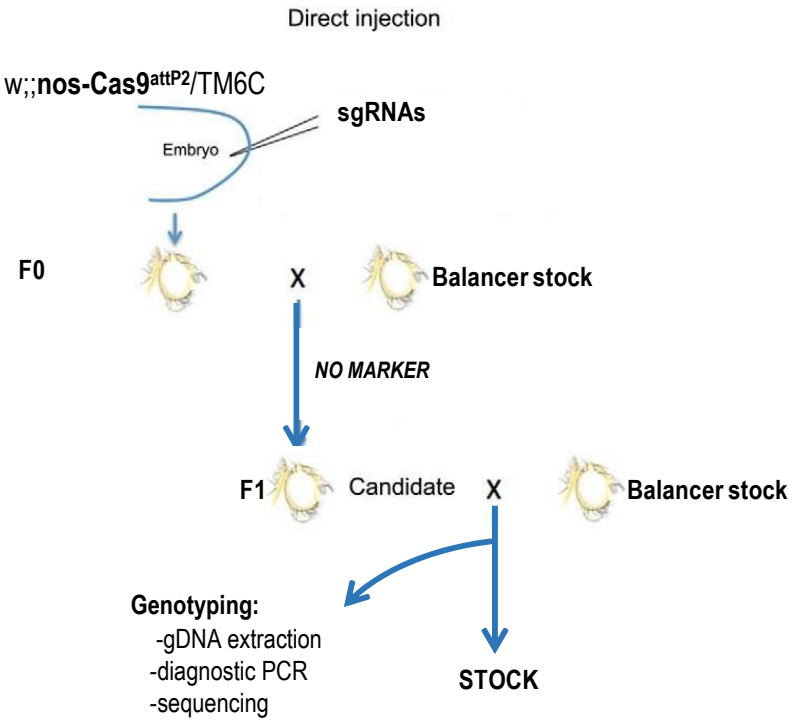

Figure 2.2 – Schematic of the strategy used for pU6-BbsI-chiRNA+sgRNA 85/86 and pU6-BbsI-chiRNA+sgRNA 87/88 injection and KO stocks selection. Adapted from Baena-Lopez et al., 2013.

Regarding the second strategy, two newly designed sgRNAs (*fu2* sgRNA -95 for the 5' end and *fu2* sgRNA -8 for the 3' end) were cloned in the same vector - pCFD5 vector (Addgene #73914) (Figure 6.1) (Nuclease et al., 2013). gDNA regions expected to be recognized by the new sgRNAs from the stock to be used for injection (Figure 2.3) were sequenced to ensure the success of gDNA-sgRNA recognition. The sequences of *fu2* sgRNA -95 and *fu2* sgRNA -8 are shown in section "6.1 – sgRNA sequences".

Subsequently, a "repair template" was created to include an attP site and a *3xpax3::mCherry* cDNA sequence flanked by loxP sequences. Both attP and mCherry are, in turn, flanked by 5' and 3' homology arms (5'HA and 3'HA respectively), homologous to the region upstream the 5' end cut and downstream the 3' end cut of the targeted locus (*fu2*). The "repair template" was inserted into pTV3 vector (Figure 6.3)

[1] Balancer stock - in this project, the balancer stock used was yw hs-flp;If/CyO; MKRS/TM6B. A balancer chromosome carries multiple inversions that suppress recombination with normal chromosomes during meiosis (Roote and Prokop, 2013).

pCFD5+sgRNAs (300ng/ µl) was co-injected with pTV3+5'HA+3'HA (500ng/ µl) in *Drosophila* embryos expressing nos-Cas9 (Bloomington 54591).

Single males from F0 generation (founder candidate flies) were crossed with balancer fly stock and the offspring of the cross was screened for the presence of red fluorescent eyes - KO candidate flies (Figure 2.3). *fu2* KO candidate stocks were established and genotyped.

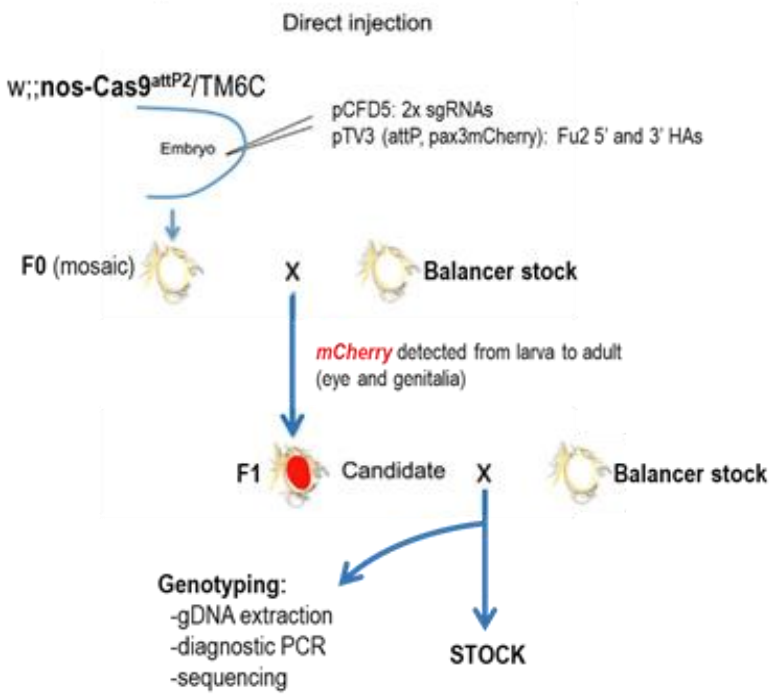

Figure 2.3 – Schematic of the strategy used for pCFD5 and pTV3 injection. Adapted from Baena-Lopez et al., 2013.

Champalimaud Foundation's Molecular and Transgenic Tools Platform (MTTP) designed the molecular strategy for *fu2* KO by CRISPR based on the existent literature of efficient CRISPR targeting (Baena-Lopez et al., 2013; Port and Bullock, 2016), with consulting from Cyrille Alexandre (Francis CRICK Institute).

The protocol used to perform the second strategy, as well as the genotyping procedures of both KO lines will be detailed in the following sub-chapters.

2.2.1 – Partial sequencing of *fu2* homology arms

sgRNA targeting region was amplified by PCR using gDNA from nos-Cas9 flies and sent for sequencing. 5'HA was amplified and sequenced using set of primers number 1 (Table 2.2) and 3'HA was amplified and sequenced using set of primers number 2 (Table 2.2).

2.2.2 – Insertion of sgRNAs into pCFD5

The design and cloning of sgRNAs into pCFD5 was performed following the cited protocol (Port and Bullock, 2016). This vector includes two BbsI restriction sites (Figure 2.4), which will be used to cut the pCFD5 and insert the sgRNAs

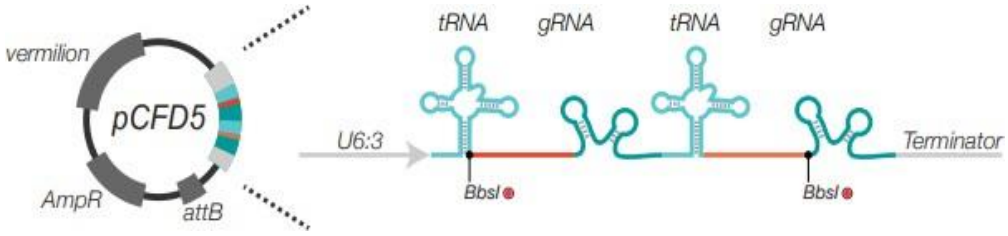

Figure 2.4 - Schematic of pCFD5 vector. It contains two BbsI restriction sites. Adapted from Port and Bullock, 2016.

sgRNA that targets *fu2* 5'HA (*fu2* sgRNA -95) was chosen considering the following criteria: avoid the ≈150 nucleotides immediately upstream from the TSS; conserved regions; cutting downstream the TSS and off-targets.

Regarding the choice of the sgRNA that targets *fu2* 3'HA (*fu2* sgRNA -8), it was taking into account that the sgRNA should recognize a sequence downstream the stop codon of *fu2*. Figure 2.5 shows the region, in the genome, for sgRNAs' recognition.

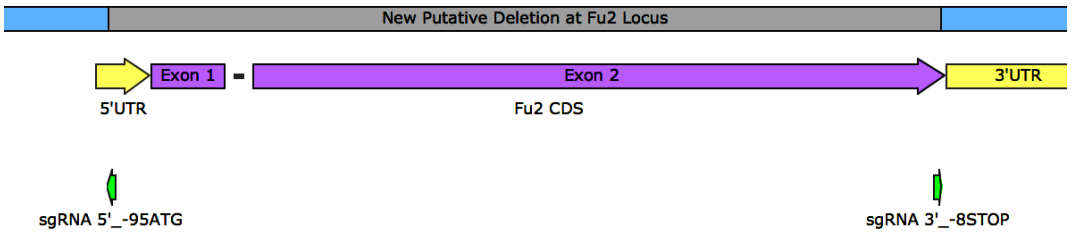

Figure 2.5 - Schematic of the targeting sites of sgRNAs in fu2 locus from nos-Cas9 flies. Sequences of both sgRNAs are represented in green arrows. fu2 sgRNA -95 recognizes one 95 bp upstream the TSS and fu2 sgRNA -8 recognizes one sequence 8 bp downstream the stop codon. The putative fragment deletion is also shown in grey.

Individual PCRs were performed, using set of primers number 3 (Table 2.2) and pCFD5 as a template, to join both sgRNA sequences in one single fragment. The PCR product was then loaded in an agarose gel and a band with 247 bp of length was extracted and purified from the gel.

The backbone was prepared by digesting 100 ng of pCFD5 with 1µL of BbsI and 3µL of its buffer in a 30µL reaction. The digestion product was loaded and run in an agarose gel and the band corresponding to the digested pCFD5 (6451 bp) was extracted and purified from the gel.

83.33 ng of fragment containing sgRNA-95 and sgRNA-8 was assembled, by Gibson Assembly, with 50 ng of digested vector, followed by a transformation step. Transformants were selected in LB agar with ampicillin (100 µg/µL).

Colony PCR was performed using set of primers number 6 to identify pCFD5+sgRNAs positive colonies. PCR product was loaded into an agarose gel and run in QIAxcel Advanced instrument. Following identification of potential positive colonies, cultures were launched and plasmid DNA from six colonies with the intended fragment length (834 bp) was extracted and sent for sequencing using U63seqfwd and pCFDseqrev. DNA from one positive colony was expanded and sent for injection.

2.2.3 – Insertion of the "repair template" into the targeting vector pTV3

To clone the homology arms into pTV3, 5'HA and 3'HA were amplified by PCR, using set of primers number 4 and 5 (Table 2.2) respectively. These primers contain restriction enzymes cut sites and sequences of the respective sgRNA + PAM. Additionally, one primer from each set also contained the PAM sequence mutated (Figure 2.6).

Figure 2.6 - Schematic of the designing of the primers for HA amplification. (A) Primers used for 5'HA amplification. (B) Primers used for 3'HA amplification. Green regions represent restriction enzyme cut sites sequences. Blue regions represent sgRNA sequences. Yellow regions represent the mutated PAM. The black portion of the primer represent the region which anneals to the DNA template. To calculate the annealing temperature of these primers it was considered only the black portion.

PCR products were analysed in an agarose gel and the bands correspondent to the 5'HA (1090 bp) and 3'HA (1065 bp) were cut and the DNA extracted.

Due to the complexity of the process, the homology arms were firstly subcloned into an intermediate vector: pCR-Blunt-II-TOPO vector (Invitrogen #K270020) (Figure 6.2)

To clone the homology arms into the vector, two DNA ligation reactions were performed: one with 5'HA and pCR-Blunt-II-TOPO vector (TOPO+5'HA) and the other one with 3'HA and pCR-Blunt-II-TOPO vector (TOPO+3'HA). For TOPO+5'HA reaction, 50ng of vector (3519 bb) was used to ligate 46.5 ng of 5'HA. For TOPO+3'HA reaction, 50ng of vector was used to ligate 45.4 ng of 5'HA. The ligation products

were transformed, and transformants were selected in LB agar with kanamycin (50 µg/µL). DNA from eight colonies from each ligation reaction was extracted and digested using PstI and loaded in an agarose gel. Plasmid DNA of two colonies from each construct which presented the right band sizes (3909 and 1400 bp for TOPO+5'HA and 4154 and 1113 bp for TOPO+3'HA) were extracted and sequenced using M13 Fw and M13 Rv primers.

After confirming the correct sequence, both homology arms were cloned into pTV3. Plasmid DNA from the colony of each ligation, which showed no mutations, was extracted and digested using NotI and NdeI (for TOPO+5'HA) and SpeI and BglII (for TOPO+3'HA). Digestion products were loaded in an agarose gel and bands corresponding to 5'HA (1090 bp) and 3'HA (1065 bp) were extracted from the gel and purified. Meanwhile, pTV3 backbone was prepared by digestion with NotI and SpeI, loading the digestion product in an agarose gel and extracting the band.

50 ng of backbone (4252 bp) was ligated to 37 ng of 5'HA. The ligation product (pTV3+5'HA) was transformed and transformants were selected in LB agar with ampicillin (100 µg/µL). Plasmid DNA from six colonies was extracted, digested with PstI and loaded in an agarose gel. The plasmid DNA of one colony which presented the right band size in the gel (3909 and 1400 bp) was digested with SpeI and BglII and ligated to 3'HA. 29 ng of 3'HA fragment (1065 bp) were ligated to 50 ng of pTV3+5'HA (5309 bp). The ligation product (pTV3+5'HA+3'HA) was transformed and transformants were selected in LB agar with ampicillin. To identify colonies pTV3+5'HA+3'HA positive, DNA from six colonies was digested using SacII and the digestion product was loaded in an agarose gel (expected bands for a positive colony: 2842 and 3482 bp). DNA from one positive colony was expanded and sent for injection.

2.2.4 – *fu2* knockout genotyping

For the KO generated by the first strategy, gDNA from *fu2* KO candidate flies was extracted and a PCR reaction was performed using set of primers number 8 (Table 2.2). PCR product was run in an agarose gel and bands with the expected size for the KO were excised, purified and sent for sequencing, using primers pBH111 and Fu2 3HA Rv.

Concerning the KO generated by the second strategy, gDNA from *fu2* founder KO candidate flies was extracted and a PCR reaction was performed using set of primers number 8 (Table 2.2). PCR product was run in an agarose gel and bands with the expected size for the KO were excised, purified and sent for sequencing, using primers pBH111 and Fu2 3HA Rv.

2.3 – *fu2* HA-tag generation

Champalimaud Foundation's MTTP designed the molecular strategy for *fu2* HA-tag generation by CRISPR based on the existent literature (Jasin et al., 2017; Li et al., 2017) and tips from the Drosophila CRISPR community.

Human influenza hemagglutinin-tag (HA-tag) was introduced to the end of *fu2* coding sequence. To do this, nos-Cas9 flies were injected with one gRNA, which recognizes a sequence 33 bp downstream of *fu2* stop codon (sgRNA 87/88), along with one oligonucleotide sequence containing 3xHA-tag and 50-60 bp Homology Arms. The oligonucleotide is one single stranded DNA sequence (ssDNA) and is composed by: 5'HA, homologous to the end of exon 2 of *fu2* (5'HA for HA-tag), 3 repeats of HA-tag (3xHA-tag), 33 nucleotides important to restore *fu2* 3'HA (3'UTR restored), mutated PAM sequence, to prevent the excision of the HA-tag through Cas9 activity and 3'HA homologous to the *fu2* 3'HA (3'HA for HA-tag). Additionally, one stop codon was created (*) in the end of the 3xHA-tag (Figure 2.7). The oligonucleotide was generated by Integrated DNA Technologies Biotechnology Company. 3xHA-tag (100ng/ µl) was co-injected with sgRNA 87/88 (150ng/ µl) in *Drosophila* embryos expressing nos-Cas9 (Bloomington 54591).

Single males from F0 generation were crossed with one balancer stock and single male flies from generation F1 were crossed again with balancer flies to establish the stock. The injection strategy is similar to the one represented in Figure 2.2 (the difference is in the injected DNA molecules). Since the oligonucleotide did not have a visible marker, the selection of the founder lines required molecular techniques (PCR and sequencing of the candidates). Consequently, when stocks were established, DNA from all the *fu2*::HA-tag candidate flies were extracted. PCR was performed using pFu2_490Fw and pBH111. PCR product was loaded in an agarose gel and the bands corresponding to *fu2*::HA-tag (838 bp) were extracted and sent for sequencing, using pFu2_490Fw and pBH111.

Figure 2.7 - Schematic of fu2 3xHA-tag oligonucleotide. Homology arms (orange regions) were added to allow homology directed repair. The 3xHA-tag consists in Human influenza hemagglutinin sequence repeated three times (green region) and it ends with one stop codon (*). Following the tag, there are 33 nucleotides to restore fu2 3'HA (blue region). The insertion sequence must also contain one mutated PAM (yellow region) to prevent Cas9 from cutting the gDNA again after HDR.

2.4 – Fly microinjection protocol

Embryos were aligned under a Leica MZ6 scope and microinjected under a Zeiss Primovert microscope adapted to microinjection, with a Narishige micromanipulator connected to a PV820 Pneumatic Picopump. Capillaries from WPI (Thin wall single- barrel Standard Borosilicate 1mm with filament) were pulled on a Sutter P-2000 needle puller to produce microinjection needles. Needles were loaded with Eppendorf Microloader™ tips.

Adult flies (nos-Cas9) were maintained in laying pots with petri dishes containing apple juice and yeast. Embryos were collected between 40min-1h after dish change and injected as soon as possible while still in a syncytial stage. For microinjection, embryos were dechorionated first with 50% bleach and aligned (around 50 per slide) all to the same side. Embryos were covered with oil 10s (VWR chemicals) to prevent dehydration but still allow gas exchanges since embryos were dechorionated. Microinjection was performed in the posterior side of the embryo, where pole cells, which later give rise to the fly gonads, are located, increasing the chances of the mutation to occur in the germ-line and being transmitted to the progeny. The DNA concentrations used for the injections varied with the experiment.

Twenty-four hours after injection, larvae were collected into a vial with food and yeast and were left 10 days at 25ºC until adult eclosion.

Injection procedures were performed by Catarina Craveiro, the technician from Champalimaud Foundation's Fly Platform.

2.5 – *Drosophila* handling

All flies were kept in a controlled chamber at 25°C with 70% of relative humidity and a light cycle where the lights were ON between 09:00 – 21:00 and OFF in the remaining hours. The food was made by Champalimaud Foundation's Fly Platform, following the Vienna Recipe (Table 6.1).

To manipulate the flies, two different scopes were used: a standard scope (Zeiss Stemi 508), for daily *Drosophila* handling, and a fluorescence microscope, Zeiss SteREO Discovery V8, to select flies with fluorescent markers. When handled, by brush or forceps, flies were kept anesthetized with carbon dioxide.

2.6 – *Drosophila melanogaster* lines

Every fly line used for this project are listed in table 2.4

*Table 2.4 - Fly lines used throughout the project and their source. Some lines were ordered from Vienna Drosophila Resource Center (VDRC) or from Bloomington Drosophila Stock Center (BL). * hs-hid is inserted in the Y chromosome.*

Fly stocks	Source
w; GMR-Gal4,UAS-Abeta$_{42}$/CyO; ;	B. Topfel
; UAS-fu2 RNAi KK line; ;	VDRC 106386
; ; UAS-fu2 RNAi TRiP line;	BL 28554
yw hs-flp; If/CyO; MKRS/TM6B;	E. Moreno
w; ; UAS-GFP dsRNA	Bl 9330
yw hs-flp; azot{KO; w}/CyO; ;	M. Martinez
w^{1118}; ; ;	E. Moreno
yw hs-flp; fu2 {KO, KI-3xpax3::mCherry 15.4}/CyO; MKRS/TM6B;	This work
yw hs-flp; fu2 KO $^{old\ guides}$ 15.6/CyO;	This work
GMR-Gal4; ; ;	C. Ribeiro
Y, hs-hid; GMR-Gal4; ; ;*	C. Ribeiro
w; UAS-Aβ$_{42;\ ;}$	D. Coelho
yw hs-flp; UAS-Aβ$_{42}$, fu2 {KO, KI-3xpax3::mCherry 15.4}/CyO; MKRS/TM6B;	This work

2.6.1 – Procedures to generate the recombinant

To test the impact of the total depletion of *fu2* in an Alzheimer's disease scenario, ;*UAS-Aβ42, fu2 {KO, KI-3xpax3::mCherry 15.4}/CyO*; recombinant was generated. To this end, homozygous female virgins from *w; UAS-Aβ42* stock was crossed with homozygous males from *ywF; fu2 {KO, KI-3xpax3::mCherry 15.4}/CyO; MKRS/TM6B* stock. In the generation F1, all the flies contained one copy of *UAS-Aβ42* and one copy of *fu2 {KO, KI-3xpax3::mCherry 15.4}*. Female virgin flies from F1 were selected and crossed with males from a balancer stock[2]. F2 generation is then screened for red fluorescent eyes, since *UAS-Aβ42* carries a mini-white marker, which restores the red color to the eyes of the flies, and *fu2 {KO, KI-3xpax3::mCherry 15.4}* carries an *mCherry* sequence, which gives fluorescence to the eyes of the flies. Single males with the intended markers are crossed with balancer female virgin flies from a balancer stock and five independent stocks were established. Figure 2.8 outlines the fly crosses required to achieve the recombinant.

[2] Female virgins are chosen instead of males, since in males meiotic crossing over does not occur (McKim and Hayashi-Hagihara, 1998). Meiotic recombination is the event that allows the joining of two transgenes in one chromatid of the progeny (Lambing et al., 2017).

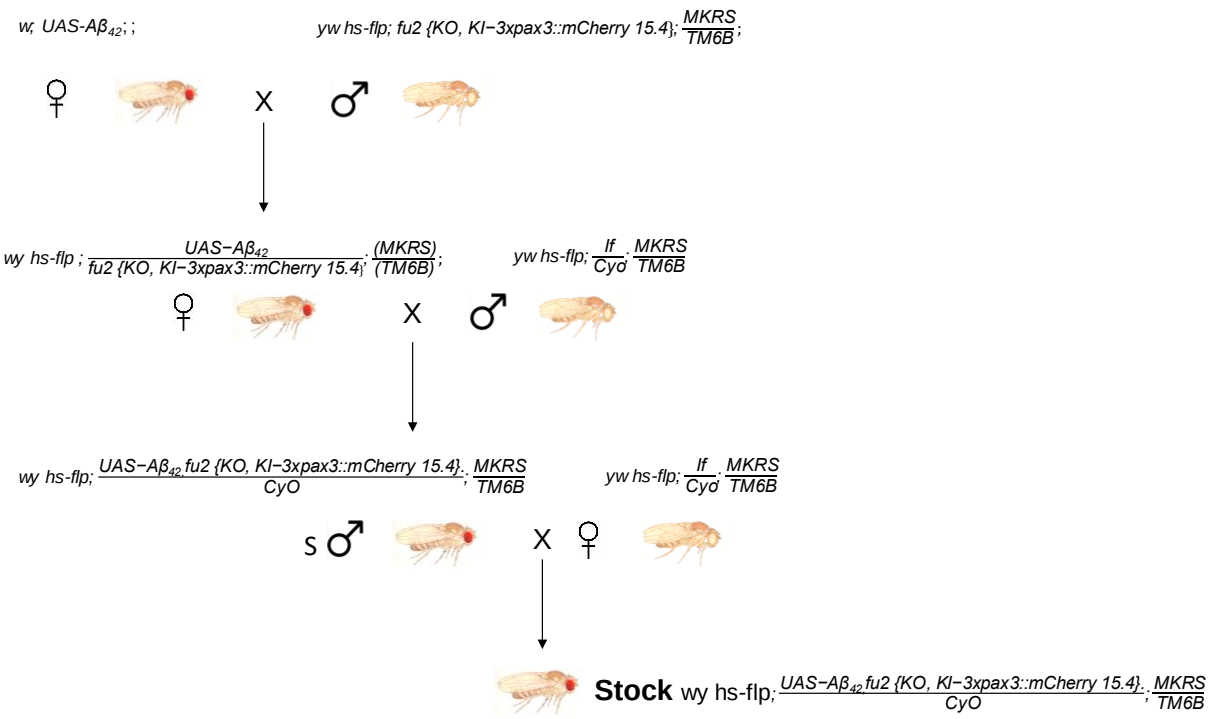

Figure 2.8 – Scheme of the crosses required to generate wy hs-flp;UAS-Aβ42, fu2 {KO, KI-3xpax3::mCherry 15.4}/CyO; MKRS/TM6B stock. Female virgins from w; UAS-Aβ42 (red eyes due to the white gene present in the construct) were crossed with ywF; fu2 {KO, KI-3xpax3::mCherry 15.4}; MKRS/TM6B (eyes with red fluorescence). To induce homologous recombination, female virgins from F1 were crossed with males from one balancer stock. From this cross, males were selected and crossed, separately, with female virgins from one balancer stock. Stocks are then established.

In order to confirm the presence of *UAS-Aβ42* transgene in the recombinant stocks, each male was separately crossed with GMR-Gal4; ; ; female virgins and the phenotype was analysed. Since *gal4* is under the control of GMR, a promoter expressed in the eye, and Aβ42 overexpression is known to promote neurodegeneration, it is expected to detect a rough-like phenotype in the adult eyes of the offspring. The presence of *fu2* KO was confirmed by PCR, using set of primers number 7 (Table 2.2).

2.7 – Dissection and Immunostaining procedures

2.7.1 – Eye imaginal discs

Third instar larvae were selected and dissected in 1x Phosphate-buffered saline (PBS). For the dissection of the larvae, the “inside out technique” was employed. The dissected samples were fixed with formaldehyde (FA) 3.7%, with agitation, for 20 minutes. After washing 3x with PBS 1x with Triton-X 0.1% (PBS-T0.1%) for 15 minutes, with agitation, the primary antibodies were incubated for 2 hours at room temperature (RT) or overnight at 4°C.Then the samples were rewashed 3x for 15 minutes in PBS-T 0.1% and incubated for 1 hour at RT with the secondary antibodies. After this incubation, samples were rewashed 2x for 10 minutes in PBS and incubated with DAPI (Sigma #D9542-5mg), with 1:1000 dilution from the stock solution at 1mg/mL, for 10 minutes. Finally, the medium was replaced by 80% glycerol and samples were mounted in one drop of 80% glycerol.

2.7.2 – Pupal retinas

Zero-hour pupae were collected and kept on a plate for 40h-42h and 42-44 hours, at 25 °C. The pupae were dissected in 1x PBS and the collected brains were fixed. The remaining procedures were similar to the previous ones (it was used PBS-T 0.4%, instead of PBS-T 0.1%).
An example of the retinas attached to the pupal brain is showed in Figure 2.9.

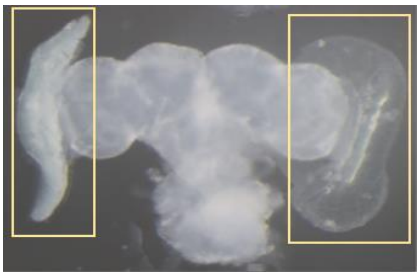

Figure 2.9 – Drosophila pupal brain. Retinas are highlighted in yellow boxes. These structures are strongly attached to the optic lobe, through a cluster of axons. Adapted from Özel et al., 2015

The list of antibodies (primary and secondary) and the respective dilution used are listed in Table 2.5. Antibodies were diluted in PBS-T. Additionally, the primary antibodies solution contained 10% of normal donkey serum (Jackson ImmunoResearch).

Table 2.5 - Antibodies required for the immunostaining protocols mentioned in the sections "2.7.1 – Eye imaginal discs" and "2.7.2 – Pupal retinas". Antibodies were diluted using PBS-T.

Antibodies	Dilution	Stock concentration (µg/mL)	Brand	Catalog number
Primary:				
Rabbit anti-cleaved *Drosophila* Dcp-1 (Asp216)	1 : 100	Unknown	Cell Signaling	#9578
Mouse anti-Elav	1 : 50	16	Developmental Studies Hybridoma Bank (DSHB)	#7E8A10
Secondary:				
Alexa Fluor 488 donkey anti-rabbit IgG	1 : 1000	1000	Invitrogen	#A-21206
Donkey anti-Mouse IgG (H+L) Secondary Antibody Alexa Fluor 647	1 : 1000	1000	Invitrogen	#A-31573
Alexa Fluor® 546 Phalloidin	1 : 200	Unknown	Molecular Probes	# A22283
Rhodamine (TRITC) AffiniPure Donkey anti-rat IgG	1 : 100	750,00	Jackson ImmunoResearch	# 712-025-153

2.8 – Confocal microscopy

To analyse all the samples of this project, confocal microscopy was used due to its advantages of high-resolution capturing sets of 2D planes in different optical sections (Z sections), without the interference of elements of adjacent Z sections. The equipment used was Zeiss LSM 880. Images were acquired with the objective Zeiss Plan-Apochromat 20x (Zeiss).

2.9 – Image Analysis

All quantifications were performed using Fiji/ImageJ. All images analysed were the result of Maximum Intensity Projections of the Z sections.

2.9.1 – Eye discs quantification

The area of differentiating neurons, behind the morphogenetic furrow, was selected. Each individualized spot of fluorescence was counted as one apoptotic cell in the selected area.

2.9.2 – Retinas quantification

Using “Region of Interest” (ROI) setting, one standard Area=2345,636µm^2, was setup in ImageJ. For each retina, three measurements were performed, always using the same ROI. The final value of each quantification is given through the mean of the three measurements performed for each retina. Each clearly individualized spot of fluorescence was counted as one apoptotic cell in the selected area.

2.10 – Statistical Analysis

Statistical analysis was performed with the software GraphPad Prism version 6.00 (GraphPad software). Statistical significance for comparison of two unpaired groups was determined using two-tailed Mann-Whitney test. Significance was defined by a P-value < 0.05. The statistical test was chosen according to the result of a normality test, also performed using GraphPad Prism version 6.00.

3 – Results

3.1 – Generation of molecular tools

Molecular tools are essential for an investigator to address the role of genes in the physiology of the organisms, by promoting the generation of transgenic flies. In this section, the main steps to create these transgenic flies will be showed.

3.1.1 – *fu2* knockout generation

In order to study the impact of the total depletion of *fu2* in different cell competition scenarios, two KO lines were generated, using two different strategies. Stock yw hs-flp; *fu2* KO$^{\text{old guides}}$ 15.6/CyO; (*fu2* KO 15.6) was generated using the first strategy described in section "2.2 – *fu2* knockout generation". Stock *yw hs-flp; fu2 {KO, KI-3xpax3::mCherry 15.4}/CyO; MKRS/TM6B; (fu2 KO 15.4)* was generated using the second strategy described in section "2.2 – *fu2* knockout generation".

3.1.1.1 – Generation of *fu2* KO 15.6

The generation of *fu2* KO 15.6 (implied the injection of two sgRNA sequences into *Drosophila* embryos. These sgRNAs recognized sequences flanking *fu2* locus, leading to the generation of DSB on those regions. Since no "repair template" was provided, gDNA will repair itself by NHEJ, generating a KO.

Upon establishment of *fu2* KO candidate stocks (injection strategy and establishment of the crosses are described in sections "2.2 – *fu2* knockout generation" and outlined in Figure 2.2), one fly from each stock was sequenced in the region of *fu2* locus. Sequencing results revealed that the coding sequence of *fu2* was successfully excised from the gDNA. This was confirmed by the absence of match between the sequenced fragment and the DNA template used for the alignment of the sequencing result (*fu2* locus). Figure 3.1 shows the sequencing result from the stock currently used in the lab.

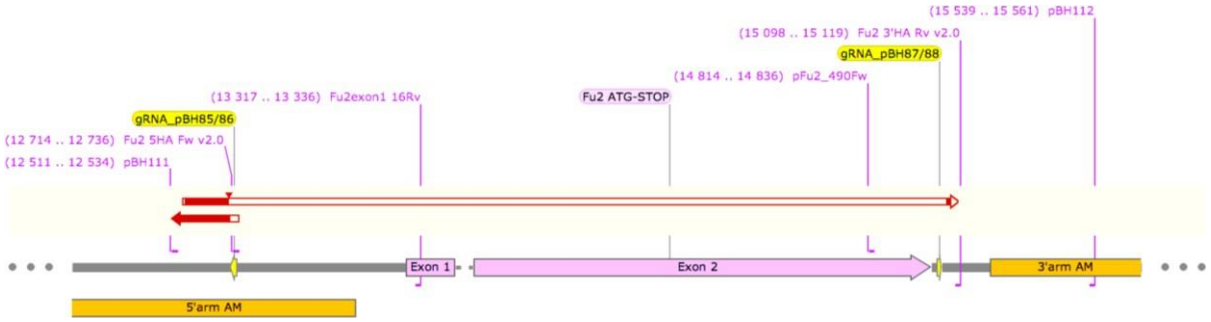

Figure 3.1 – Alignment of fu2 locus sequencing (arrows) with fu2 locus DNA template (bottom sequence). White regions from the two arrows on the top show unmatched regions between the sequenced fragment and the DNA template. Red regions of the arrows show matched regions between the sequenced fragment and the DNA template.

3.1.1.1.1 – Fly microinjection

Concerning the injection procedures to generate this KO, a total of 1284 embryos were injected, of which only 340 larvae were collected. From these larvae, 81 reached adult stage (41 females and 40 males). Only male flies were crossed, with balanced flies, and 15 of them were sterile. 25 crosses generated F1 and, upon genotyping, only one founder KO line was identified. Therefore, the efficiency of the strategy was 0.08% (1/1284).

3.1.1.2 – Generation of *fu2* KO 15.4

To generate *fu2* KO 15.4, two sgRNAs and one "repair template" were co-injected in *Drosophila* embryos. The sgRNAs will lead to the generation of DSB and the cell's endogenous mechanisms for DNA repair use the "repair template" to restore the cut region, by inserting attP and *3xpax3::mCherry* sequences into *fu2* locus, through homology directed repair (HDR) (Figure 3.2 A). This is possible due to the presence of HA in the "repair template". To linearize the "repair template", sgRNA+PAM sequences were added to the ends of the "repair template", which allows for Cas9 to cut the gDNA and the "repair template", avoiding the injection of an extra vector coding for a restriction enzyme.

fu2 KO 15.4 flies can be easily identified by the presence of the marker mCherry in the eyes and central nervous system, since *mCherry* is being controlled by 3 repetitions of a promoter expressed in the neuronal cells (3x*pax3*).

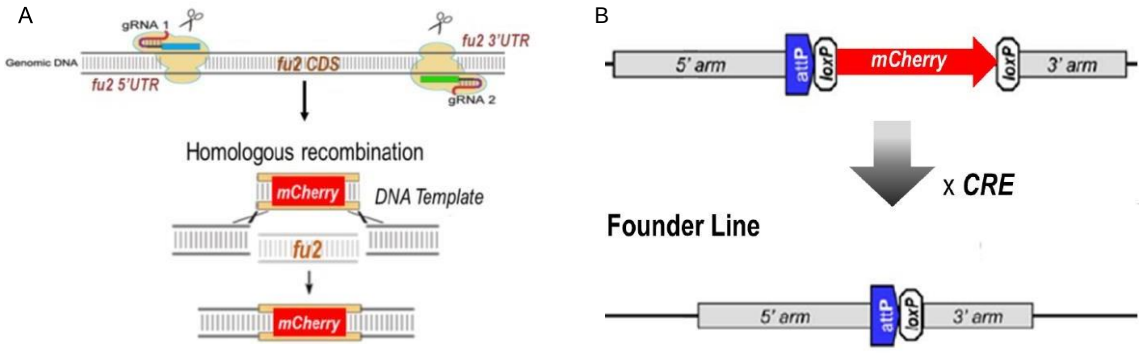

Figure 3.2 – Strategy to generate fu2 KO 15.4 and posterior knock-in induction (A) - Schematic of the strategy to generate fu2 KO 15.4 (insertion of attP is not shown). (B) – Excision of mCherry sequence, using cre recombinase. Adapted from (Huang et al., 2009) *and from flycrispr website.*

Upon establishment of the stocks, *3xpax3::mCherry* marker can be removed from the gDNA of the fly, by crossing this KO flies with flies expressing a Cre recombinase, which will remove the region between the loxP sequences (in this case, *mCherry* sequence) (Figure 3.2 B). A simple schematic of the repair template is represented in figure 3.3.

Figure 3.3 – Simplified representation of DNA "repair template" used for HDR. 5'HA and 3'HA are homologous to the regions upstream and downstream the cut sites, mCherry is under the control of a promoter expressed in the neurons (3xpax3) and both sequences (3xpax3 and mCherry) are flanked by loxP sequences. Upon the action of a Cre recombinase, only attP site will remain in the fu2 locus, allowing posterior knock-in generation. sgRNA+PAM sequences were added to the ends of the "repair template" to induce the cut by as9.

3.1.1.2.1 – Single-nucleotide polymorphism Analysis

Before advancing to the molecular cloning steps, there was the need to sequence the region recognized by *fu2* sgRNA -95 and by *fu2* sgRNA -8. The aim was to identify the presence of putative single-nucleotide polymorphisms (SNPs) in the genomic targeting region of nos-Cas9 flies. The sequencing results from a region of 5'HA and 3'HA showed that, although some SNPs were detected mainly in the 3'HA (vertical red bars in Figure 3.4), no difference is identified in the genomic targeting region for the sgRNAs (green arrows of Figure 3.4), compared to the sequence existing in Flybase website (http://flybase.org/). This means that the sgRNA targeting sequence is the same in nos-Cas9 gDNA and in the sequence present in the databases. Therefore, the designed sgRNAs may be used to induce DSB in the region of interest.

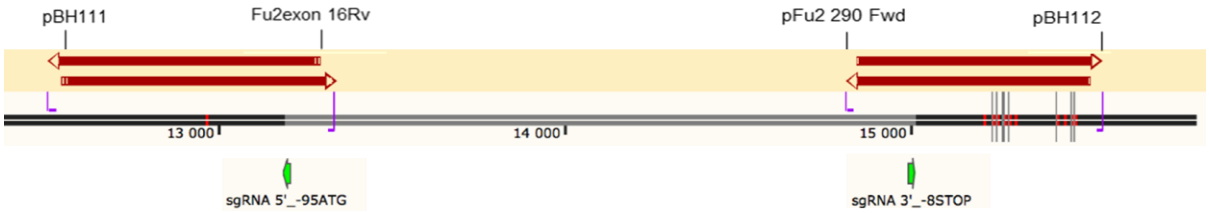

Figure 3.4- Alignment of fu2 homology arms partial sequencing to fu2 locus template. The horizontal red bars show alignment of sequenced region to the genome. The vertical red bars on top of the black line show the differences of nucleotides observed between the sequenced region and the annotated locus sequence. Green arrows represent the recognition region of sgRNAs in the genome. Note that neither 5'HA nor 3'HA were completely sequenced.

3.1.1.2.2 – Cloning of sgRNAs in pCFD5

To reduce the amount of injected DNA, both sgRNAs were cloned into the same vector (pCFD5). To this end, both sgRNA sequences were joined together in one single fragment, through PCR, using pCFD5 as DNA template. Then, one Gibson Assembly (GA) was performed to join the fragment containing the sgRNAs to digested pCFD5 vector (Figure 3.5). The sgRNA sequences are represented in orange squares in Figure 3.5.

For GA to be successful, the fragment with the sgRNAs contained ends (black regions of the fragment in Figure 3.5) that overlapped with the ends generated by the digestion of pCFD5.

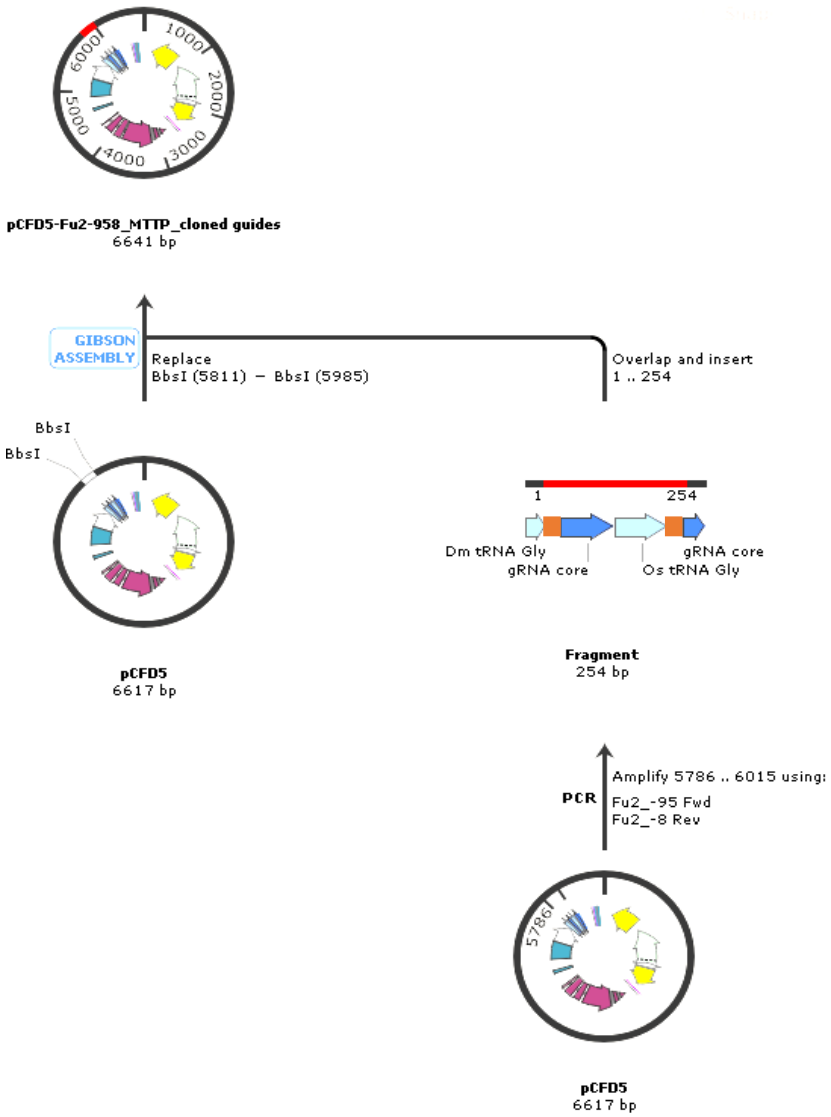

Figure 3.5 - Schematic of sgRNA cloning in pCFD5, read from bottom to top. Primers containing sgRNAs were joined together through PCR, using pCFD5 as template. The backbone is digested using BbsI restriction enzyme and the fragment is inserted in the vector through Gibson Assembly (note that the grey portions in both ends of the fragment overlaps with the ends of pCFD5). The fragment contains not only the sgRNAs sequences, but also the region excised from pCFD5 upon BbsI enzymatic digestion (gRNA core and Os tRNA Gly).

Since GA reaction is not 100% efficiency, and its efficiency is inversely proportional to the fragment's length (Gibson Assembly® Master Mix Instruction Manual), there was the need to confirm that the sgRNAs were inserted correctly and without mutations. The fragment containing both sgRNAs, from six different colonies, was sequenced. Sequencing results showed the absence of mutations in three independent colonies (colonies number 3, 7 and 9 from Figure 3.6). The detailed protocol for cloning both sgRNAs is described in section "2.2.2 – Insertion of sgRNAs into pCFD5".

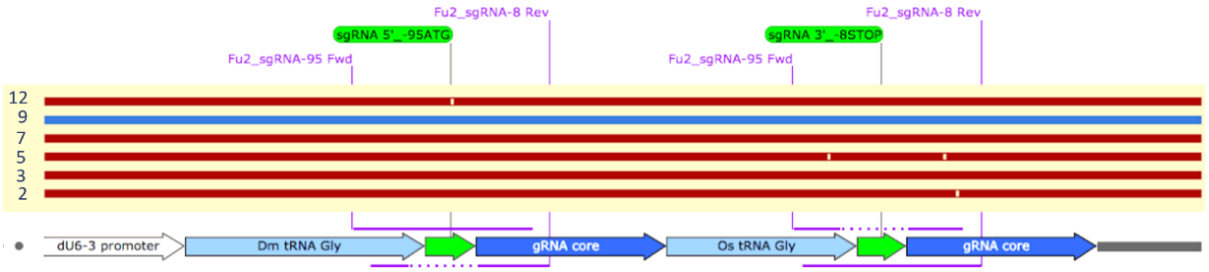

Figure 3.6 - Alignment of sequenced fragments to pCFD5 containing sgRNAs sequences. Each line represents sequenced results from colonies number 12, 9, 7, 5, 3 and 2. The red bars represent the portion of DNA that matches to the template DNA. White gaps along the sequenced fragments represent mutations compared to the template sequence (bottom sequence) or sequencing errors. The blue line represents the sequence from the colony chosen for further DNA amplification. Green arrows (in the template DNA) represent the sgRNA sequences.

3.1.1.2.3 – Cloning of "repair template" in pTV3

Upon the induction of DSB, one "repair template" is used to repair the damage. This was possible due to the presence of HA flanking the insertion sequence (attP and *mCherry*). To clone the "repair template", 5'HA and 3'HA were firstly amplified from gDNA of nos-Cas9 flies, using specific primers that add restriction sites in the ends of the fragments. Once amplified, fragments were cloned in an intermediate vector (pCR-Blunt- II-TOPO). Although the homology arms were cloned in separate pCR- Blunt-II-TOPO vectors, the general cloning strategy was similar for both homology arms (Figure 3.7).

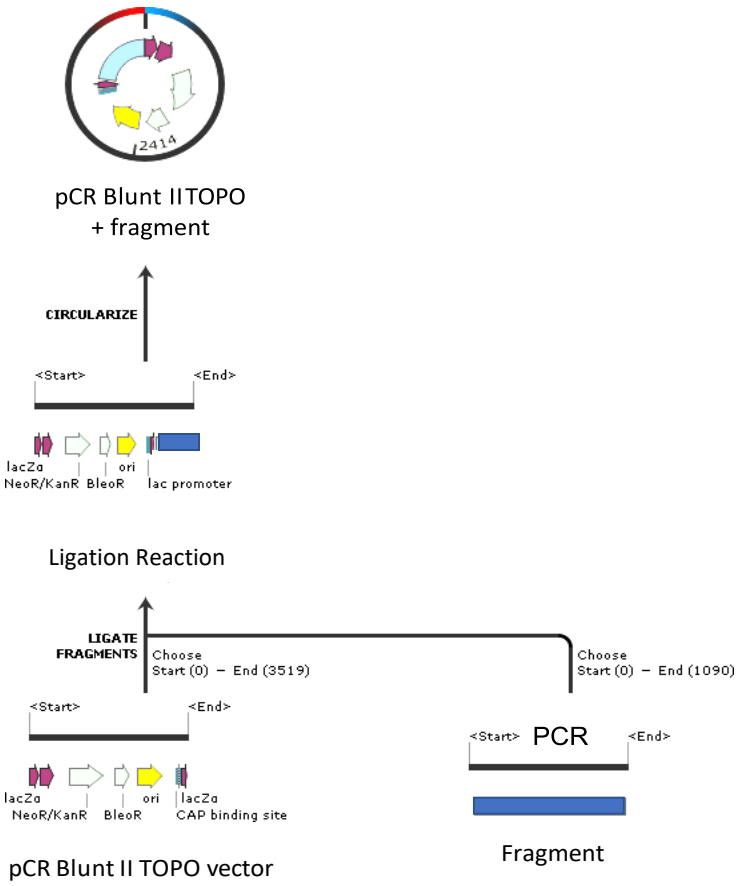

Figure 3.7 - Schematic of the general cloning strategy for homology arms cloning in pCR-Blunt-II-TOPO, read from bottom to top. Each HA (fragment) was amplified by PCR and then ligated in separate pCR Blunt II TOPO vector (ligation reaction).

To ensure that the 5'HA and the 3'HA did not suffer mutations during the cloning process, both regions were sequenced. The sequencing results (Figure 3.8) show some mutations common to all the sequenced fragments, suggesting that the gDNA from nos-Cas9 might differ, in some nucleotides, from the annotated sequence present in the databases.

A

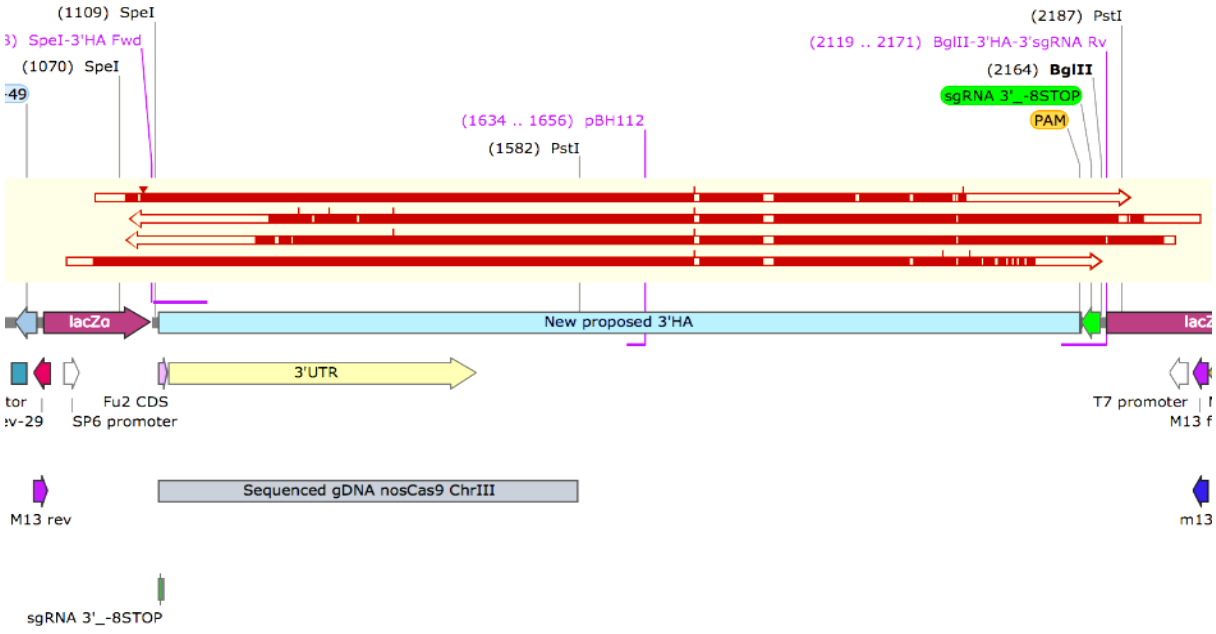

B

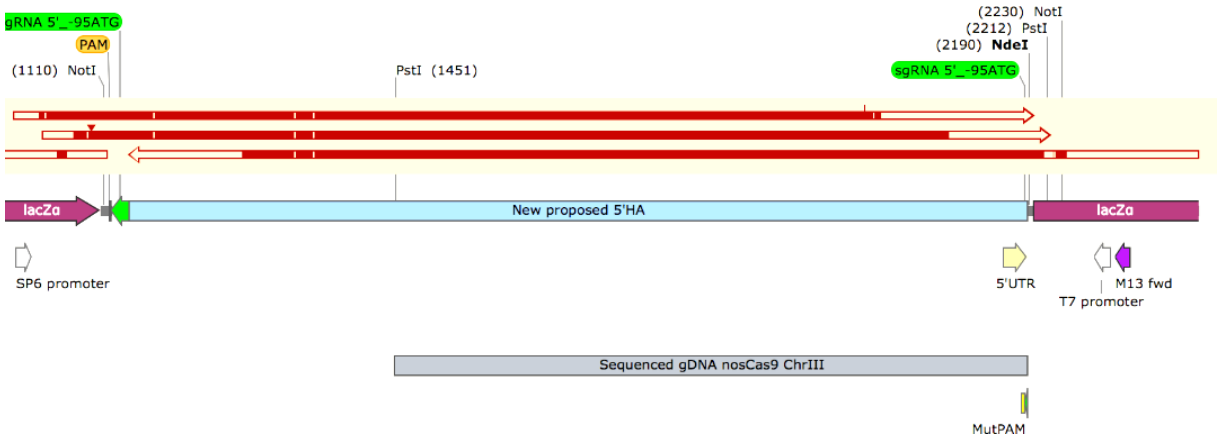

Figure 3.8 - Alignment of sequenced fragments (arrows) to pCR-Blunt-II-TOPO vector containing 5'HA or 3'HA sequences (bottom sequences). Two colonies from each ligation were sequenced. (A)- Sequencing of 3'HA. This homology arm includes regions downstream of fu2 3' untranslated region (3'UTR). The genomic PAM sequence is replaced by one mutated PAM. (B)- Sequencing of 5'HA. This homology arm includes a considerable region upstream of fu2 5' untranslated region (5'UTR). The PA existing in the genome is replaced by one mutated PAM sequence. The red bars represent the portion of DNA that matches to the template DNA. White gaps along the sequenced fragments represent unmatched regions the template sequence.

Both fragments were then excised from the respective pCR-Blunt-II-TOPO vectors and ligated, sequentially, to pTV3 vector (Figure 3.9).

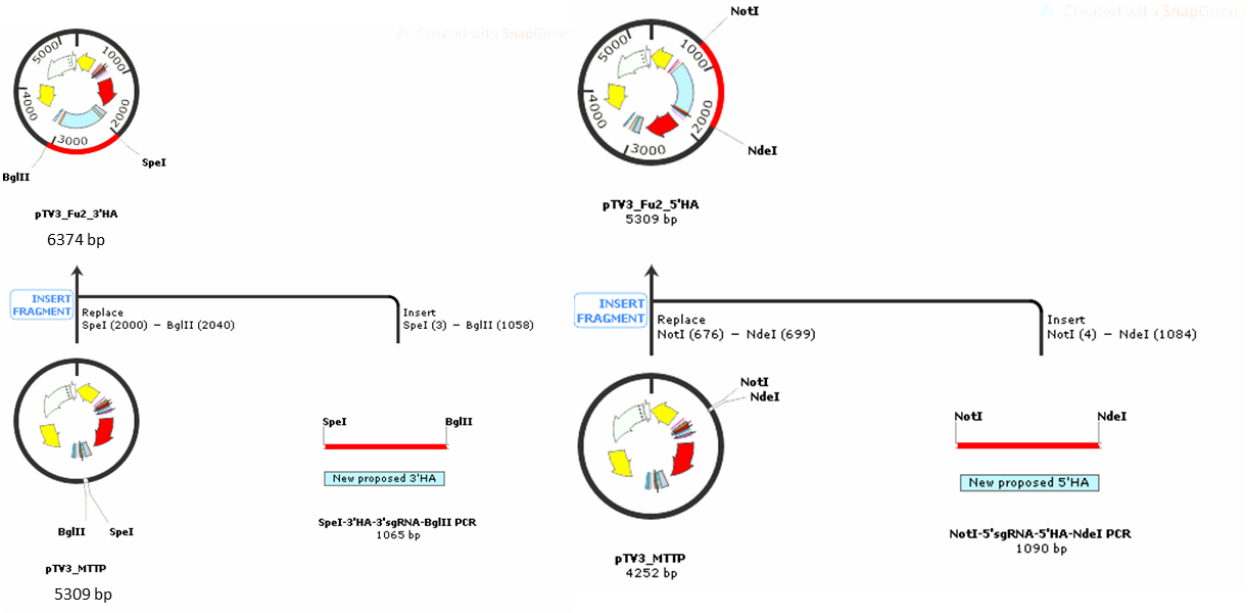

Figure 3.9- Schematic of homology arms cloning in TV3, read from bottom to top. Excised fragments were ligated sequentially to the final vector (pTV3). Firstly, 5'HA was ligated to pTV3 digested with NotI and NdeI, generating a vector with 4252 bp long (pTV3+5'HA), and then, 3'HA was ligated to pTV3+5'HA digested with SpeI and BglII, generating the final pTV3+5'HA+3'HA vector (6374 bp).

3.1.1.2.4 – Fly microinjection

The injection of pTV3+pCFD5 was performed in a total of 470 embryos, of which 197 larvae were collected. From these larvae, only 57 reached adult stage (30 females and 27 males). Only male flies were used to cross with balancer flies and 4 of them were sterile. When the screening for red fluorescent eyes was performed, only 5 founder KO lines were identified. Therefore, the efficiency of the strategy was 1% (5/470).

3.1.1.2.5 – *fu2* knockout genotyping

To assure that attP sequence is inserted in the correct region, *fu2* locus from KO candidate stocks was amplified using one primer upstream the *fu2* 5'HA and one primer downstream *fu2* 3'HA and then sequenced. Sequencing results (Figure 3.10) reveal that the amplified fragment contained attP, followed by *mCherry* sequence, proving that the insertion of attP in *fu2* locus was successful.

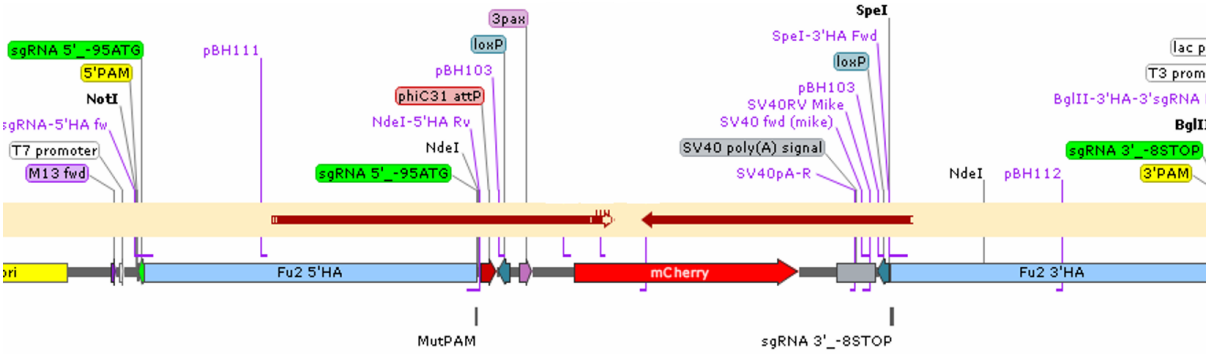

Figure 3.10 - Alignment of sequenced fragment (arrows) to pTV3+5'HA+3'HA DNA template (bottom sequence). The region of interest (attP- red box) is inserted in the gDNA (demonstrated by the red arrows, which means that there is a match between the sequenced fragment and the DNA template). The sequencing result of only one line is shown, to simplify the figure.

3.1.1.3 – Phenotypic analysis of the knockout lines

Upon establishing of the stocks, some phenotypical characteristics were observed:

1. In *fu2* KO 15.6 line, some homozygous flies show wings slightly curved down. However, the phenotype is not visible in all homozygous flies, which shows that it does not have a penetrance of 100% or the existence of off-target effects.
2. In *fu2* KO 15.4 line, there is a significant difference in the Mendelian ratio. The Mendelian ratio is defined as the ratio of progeny with a specific phenotype or genotype expected in accordance with the Mendel law (mendelian ratio. (n.d.) *Farlex Partner Medical Dictionary*. (2012)). Hence, when two heterozygous KO 15.4 flies are crossed, it is expected to have 33.3% of homozygous KO 15.4 flies (1/3 x 100= 33.3), according to Mendel law, and taking into account that flies *CyO* homozygous are lethal (Table 3.1). However, only 8.22% of flies are identified as homozygous (6 homozygous flies/73 total flies x 100= 8.22). This result suggests a transmission ratio distortion, where an allele is preferentially transmitted to the offspring (Huang et al., 2013).

Table 3.1 – Mendelian ratio of the progeny resulting from crossing two flies fu2 {KO, KI-3xpax3::mCherry 15.4}/CyO. One of the resultant genotypes is lethal. Hence, it is not taken into account when the Mendelian ratio is calculated.

Male / **Female**	*fu2* KO 15.4	*CyO*
fu2 KO 15.4	*fu2* KO 15.4 HZ	*fu2* KO 15.4/ *CyO*
CyO	*fu2* KO 15.4/ CyO	~~*CyO*/*CyO*~~

3. Both KO lines are homozygous viable.

3.1.2 – *fu2*::3xHA-tag generation

In addition to the knockout's generation, one KI (*fu2::*3xHA-tag) was created to address the expression of *fu2* in tissues. This was performed by inducing one DSB at *fu2* 3' HA (using one sgRNA which recognizes a region in *fu2* 3'HA). Then, one oligonucleotide was designed to include homology arms, homologous to the region upstream and downstream the cut site. With this strategy, 3xHA-tag was inserted in the gDNA of the flies, leading to the co-expression of *fu2* and 3xHA-tag. The oligonucleotide

was injected in flies as a single-strand molecule. More details about the oligo design and the KI generation are present in section “2.3 – *fu2* HA-tag generation”.

3.1.2.1 – Fly microinjection

After 4 injection attempts of the oligonucleotide with sgRNA 87/88, from the 580 injected embryos, 219 larvae were collected and from these larvae, only 34 flies reached adult stage (17 males and 17 females).

All males were crossed, separately, with a balancer stock, generating *fu2*::3xHA-tag candidate stocks.

3.1.2.2 – *fu2*::3xHA-tag genotyping

Since the inserted fragment did not contain a visible marker, there was the need to perform a genotyping screening to ensure the HA-tag was correctly inserted in the 3’ end of *fu2*. Hence, upon establishment of the stocks, DNA from the injected flies was sequenced. Sequencing results (Figure 3.11) revealed the insertion of an unidentified sequence. This sequence led to the generation of a stop codon in the beginning of the first HA-tag sequence, probably due to frameshift effects. Additionally, only one of the HA repetitions is recognized. The sequencing results also revealed the successful insertion of the mutated PAM sequence. Due to the fact the mutated PAM is inserted in the 3’HA of the oligonucleotide, it is possible to conclude that HDR occurred with success. The genotyping screening revealed the existence of one founder line. However, the insertion of the unidentified sequence and the generation of a stop codon turned *fu2::3xHAtag* impracticable to be used in further experiments.

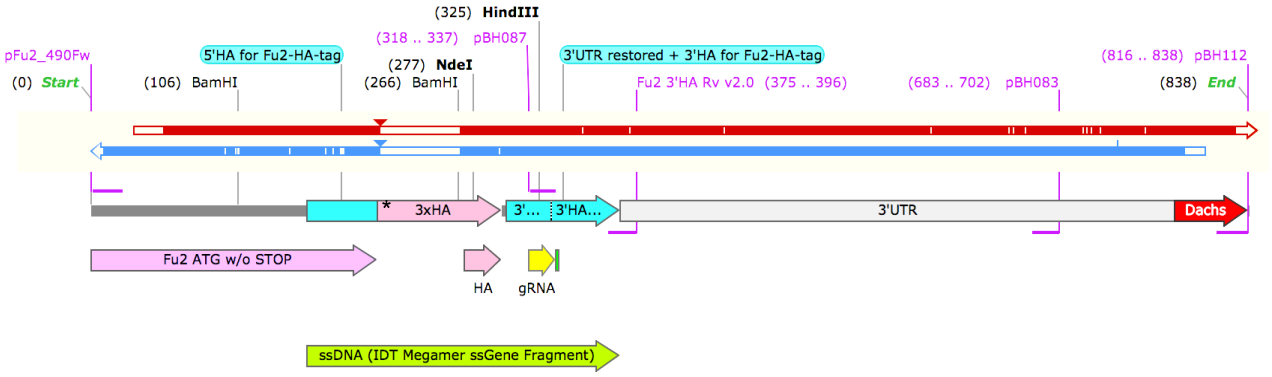

Figure 3.11 – Alignment of sequenced fragment (arrows) to the template DNA of fu2::3xHA-tag (bottom sequence). The gDNA sequenced contains an unknown sequence replacing two Human influenza hemagglutinin sequences. One sequence of Human influenza hemagglutinin and the mutated PAM were inserted successfully. One stop codon (*) was generated in the ending of the coding sequence of fu2.

3.1.2.3 – Strategy efficiency

Since only one founder line was generated from the 518 injected, the strategy efficiency is 0.17% (1/580).

3.2 – The role of *fu2* in Alzheimer's disease

These set of experiments were planned after Dr. Dina Coelho, a post-doc fellow in the laboratory, have showed that approximately 60% of cell death induced by $A\beta_{42}$, in the eye imaginal discs, was flower-dependent (Coelho *et al., in preparation*). Since *fu2* was found to be expressed in loser cells, the goal of these set of experiments is to understand if *fu2* is required for *fwe*-dependent loser cell elimination in Alzheimer's disease.

To this end, while *fu2* KO lines were being generated, *RNAi* lines were used to induce the downregulation of *fu2*. Flies containing *UAS-fu2 RNAi* were crossed with flies overexpressing $A\beta_{42}$ in the differentiating retina (posterior to the morphogenetic furrow). The expression of $A\beta_{42}$ in this specific region is assured by *GMR* promoter (*GMR> $A\beta_{42}$)*. Two *fu2* RNAi lines were used for this experiment: *UAS-fu2 RNAi* TRiP line and *UAS-fu2 RNAi* KK line.

Discs were stained with Dcp-1 (green) to analyse the level of apoptosis, Elav (grey) to label photoreceptors, phalloidin (magenta) to stain F-actin (a component of the cytoskeleton) and outline the cells and DAPI (blue) to show the nuclei of the cells.

The positive control, overexpressing $A\beta_{42}$ (*GMR-Gal4, UAS-$A\beta_{42}$/ UAS-GFP dsRNA*) presented high levels of apoptosis, evidenced by the presence of a high number of Dcp-1 positive cells (Figure 3.12 A, D). When $A\beta_{42}$ was co-expressed with *UAS-fu2 RNAi*, different results were obtained, according to the RNAi line used. w; *GMR-Gal4, UAS- $A\beta_{42}$ / UAS-fu2 RNAi KK* line did not show a significant difference in cell death compared to the control (Figure 3.12 B, D). However, w; *GMR-Gal4, UAS- $A\beta_{42}$/ +; UAS-fu2 RNAi* TRiP line/ + showed higher levels of apoptosis (Figure 3.12 C), which is reflected by an increase of Dcp-1 positive cells (Figure 3.12 D).

Since the two RNAi lines (KK line and TRiP line) reveal different levels of cell death, these results need to be confirmed using the KO lines generated to ensure the complete absence of *fu2* contribution and rule out the strength of the RNAi lines as a source of this differential results.

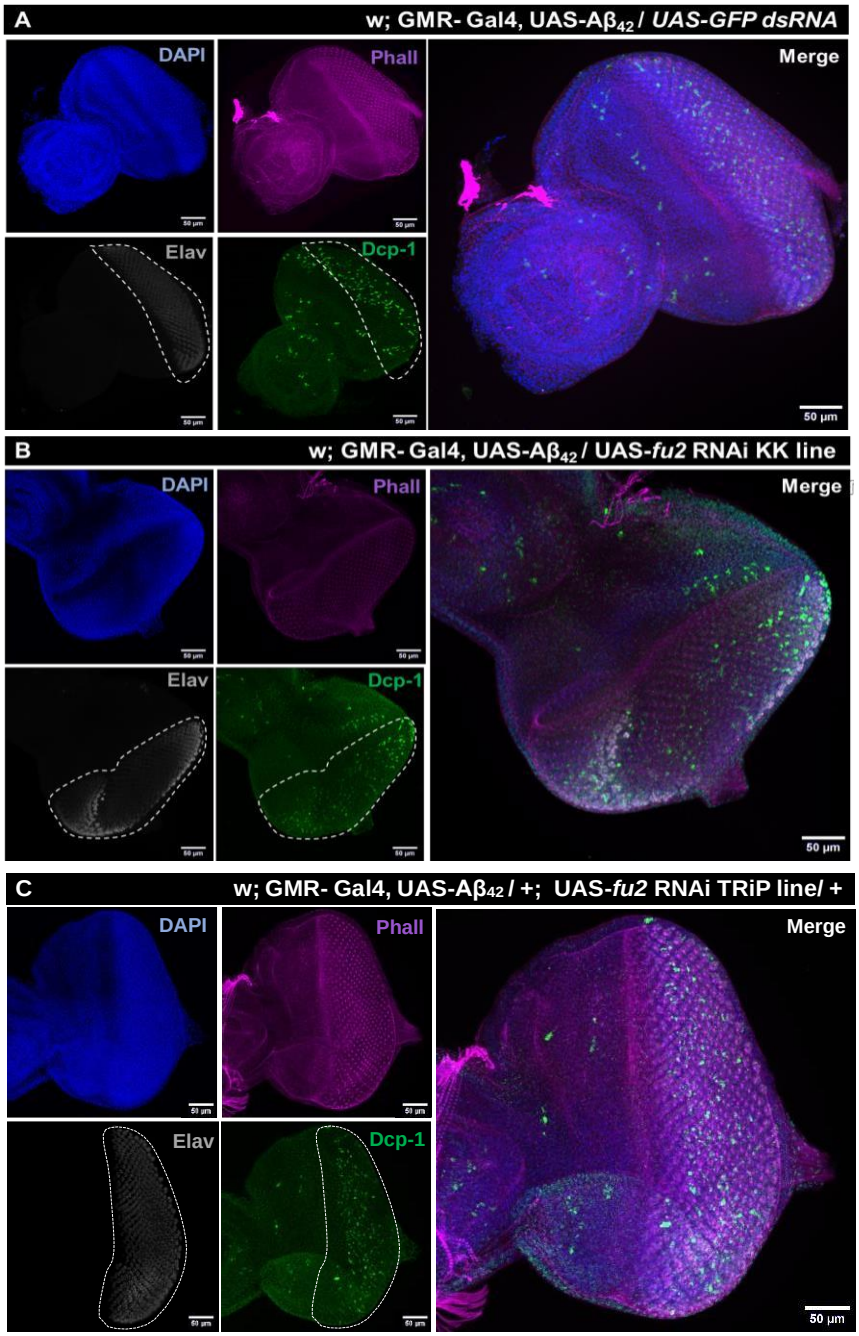

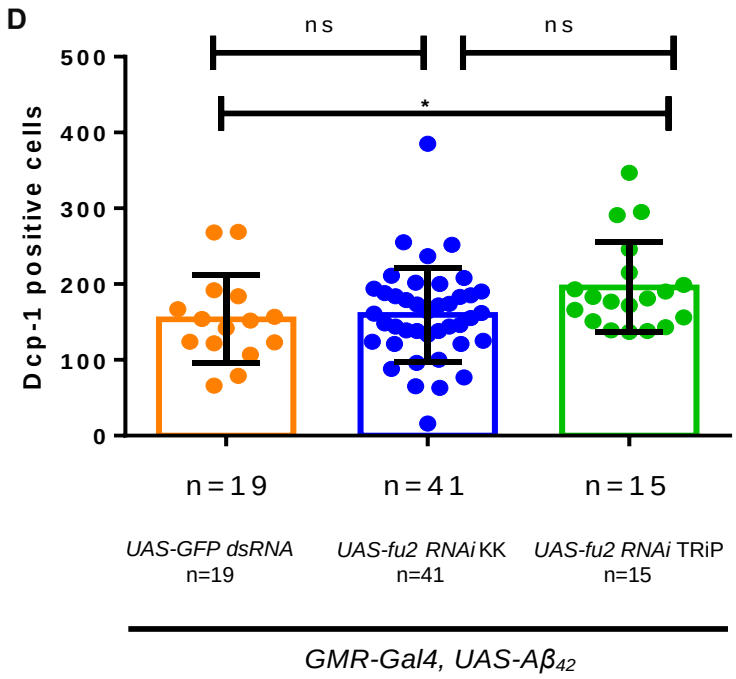

Figure 3.12 – fu2 might be involved in cell elimination in a context of Alzheimer's disease (A), (B), (C) – Eye discs stained with DAPI (in blue), Dcp-1 (in green), Elav (in grey) and Palloidin (Phall; in magenta). The area involved by the with dashes represent the area of Aβ42 expression (quantified area) (D) - Number of dying cells (Dcp1 positive cells) in a context where fu2 is being downregulated, in an Alzheimer's disease context, using two different RNAi lines against fu2: KK (blue) and TRiP (green). The control is represented in orange. The area analysed corresponds to the differentiated neurons (dashed area). n - number of eye discs analysed; (*)-p≤0.05; ns – not signifative.

3.2.1 – Recombinant generation

In order to assess more accurately the role of *fu2* in Alzheimer's disease, a recombinant line was created: yw hs-flp*; UAS-Aβ42, fu2 {KO, KI-3xpax3::mCherry 15.4}/CyO; MKRS/TM6B*. The steps to generate the recombinant line are described in "2.6.1 – Procedures to generate the recombinant".

The presence of both sequences (*UAS-Aβ42* and *fu2* KO 15.4) in the recombinant was confirmed by crossing the recombinant lines with flies expressing GMR-Gal4. Lines containing and expressing *UAS*-Aβ42 displayed an eye degeneration phenotype associated with the overexpression of the Aβ42 in the retina (Figure 3.13 E), which is not visible in flies where *UAS*-Aβ42 is not expressed (Figure 3.13 A, B, C, D).

The presence of *fu2* was followed by the expression of *mCherry* corresponding to *3xpax3::mCherry* insertion in *fu2* locus (Figure 3.13 E'). A gradual decrease in fluorescence is visible from the homozygous KO stock (Figure 3.13 C') to the heterozygous recombinant (Figure 3.13 D') and from this one to the recombinant expressing Aβ42 (Figure 3.13 E').

In addition, the presence of *fu2* was determined by a PCR, performed in heterozygous recombinant candidate stocks. PCR result showed the presence of a fragment with the size of *mCherry* (2098 bp) and a fragment with the WT band size (2609 bp) (Figure 3.14)

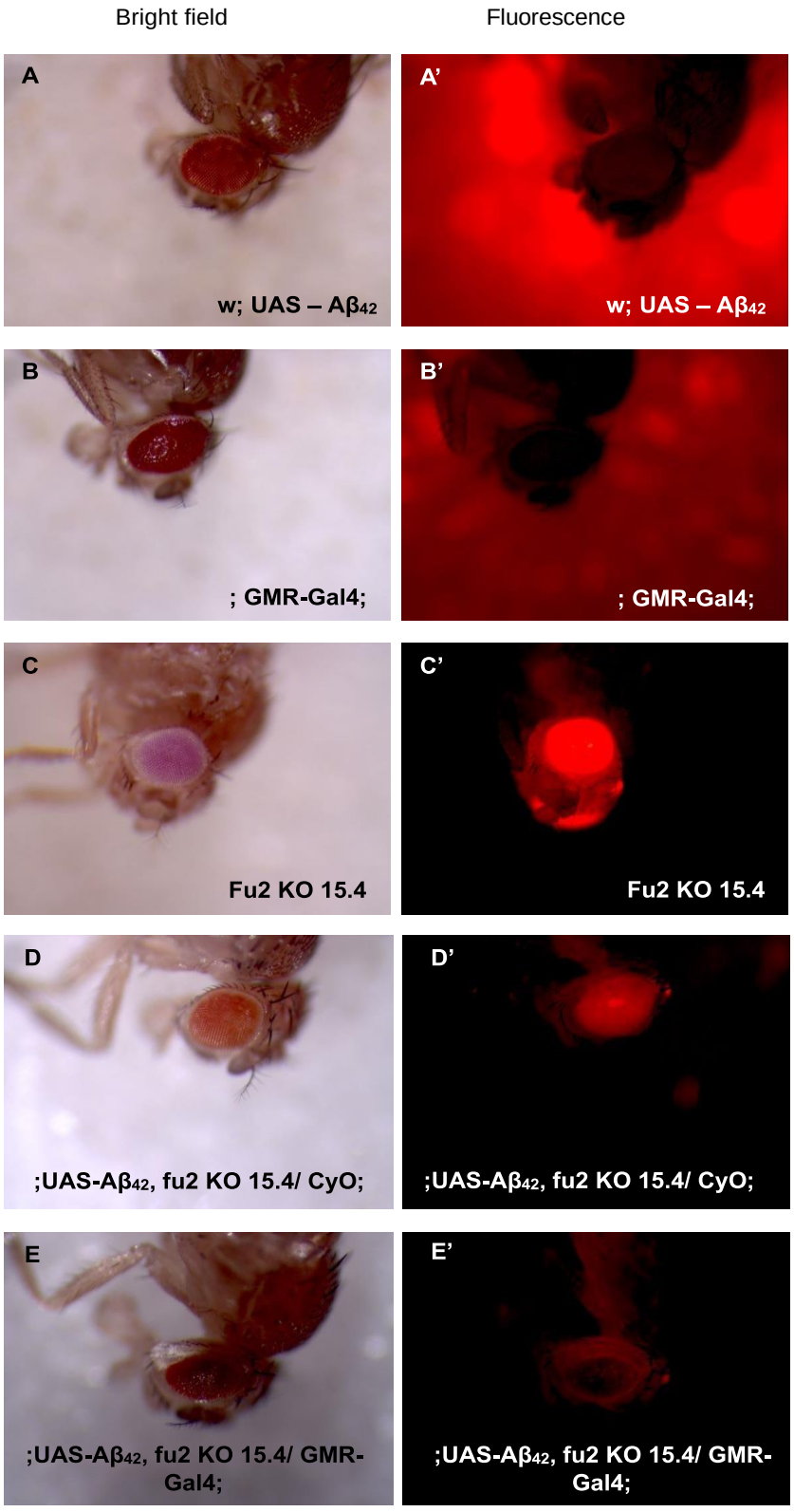

Figure 3.13 – Confirmation of [UAS Aβ42, fu2 KO 5.4] recombinants by mCherry presence. Flies were first screened for the area of the eye in brightfield (A, B, C, D and E) and then, for the presence of mCherry, under red fluorescence (A', B', ', D', E'). (A-D) – Controls. Fu2 KO 15.4 corresponds to the stock ywF; fu2 {KO, KI- 3xpax3::mCherry 15.4}/CyO; MKRS/TM6B. UAS- Aβ42, Fu2 KO 15.4/CyO represents the recombinant genotype
(E) – Recombinant overexpressing Aβ42. The decrease in fluorescence when Aβ42 is expressed is visible.

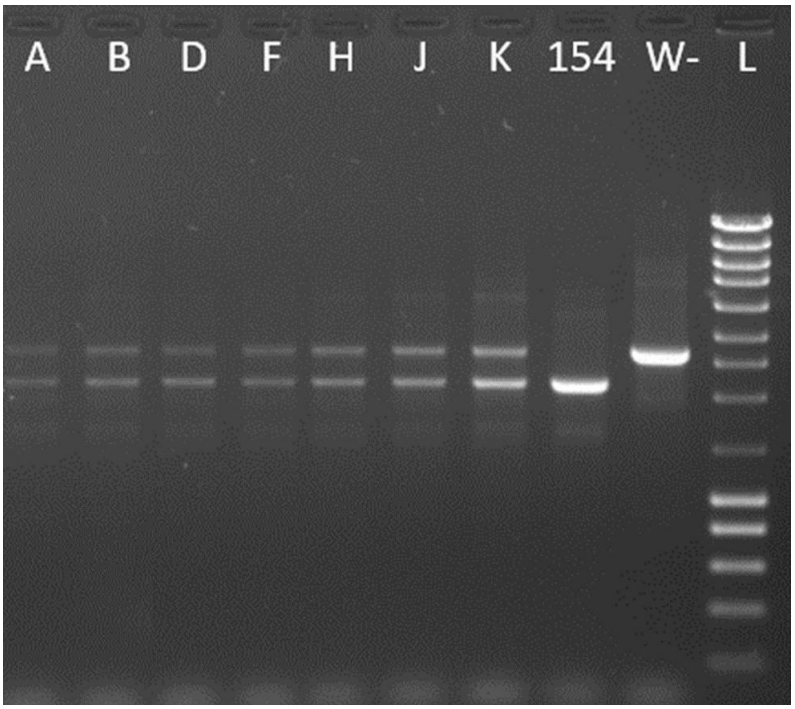

Figure 3.14 – Confirmation of [UAS-Aβ42, fu2 KO 5.4] recombinants by P R. Agarose gel from the PCR result of UAS-Aβ42, fu2 KO 15.4 recombinant candidate lines (A-, B, D, F, H, J, K). 154- positive control. w - - negative control. L- NZYDNA DNA Ladder III.

3.3 – The role of *fu2* during neuronal culling

Another cell competition context tested in this project was the neuronal culling, a mechanism that allows the elimination of supernumerary neurons in the periphery of the retina during pupae formation.

To test if *fu2* is required for the elimination of these neurons, cell death in retinas of *fu2 KO*$^{old\ guides}$ *15.6* stock was analysed. Two controls were used in this experiment: a positive control (w^{1118} stock) and a negative control (*ywF; azot{KO; w}* stock). Two timepoints were analysed: 40h-42h after pupae formation (APF) and 42h-44h APF and Dcp-1 positive cells were quantified on the edge of the retinas. Together with Dcp-1, retinas were stained with the pan-neuronal marker Elav, to label the photoreceptors and DAPI to show the nuclei of cells.

Results show that there is an overall decrease in Dcp-1 positive cells over time, which may suggest that the intensity of cell death decreases overtime. This decrease is most significant in both controls (w^{1118} and *azot KO* stocks) (Figure 3.15 A, B, D). Also, when the amount of cell death in the three genotypes tested of the same timepoint is compared (40h-42h APF or 42h-44h APF), no significant difference is identified (Figure 3.15 D).

Regarding *fu2* KO stock, the results are inconclusive, since the two controls show the same amount of cell death (Figure 3.15 A, B, C, D).

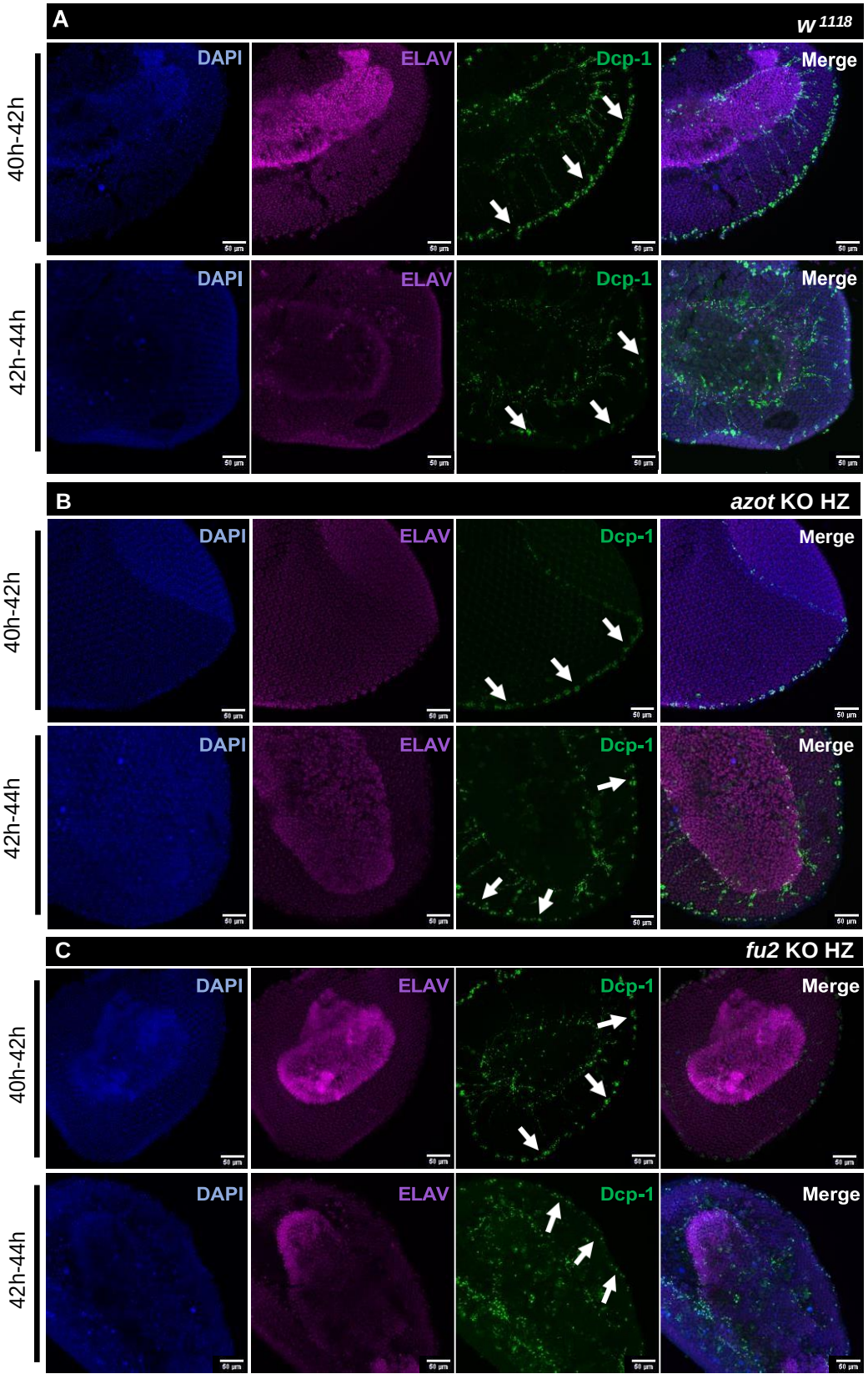
A
w 1118
40h-42h
DAPI
ELAV
Dcp-1
Merge
42h-44h
DAPI
ELAV
Dcp-1
Merge
B
azot KO HZ
40h-42h
DAPI
ELAV
Dcp-1
Merge
42h-44h
DAPI
ELAV
Dcp-1
Merge
C
fu2 KO HZ
40h-42h
DAPI
ELAV
Dcp-1
Merge
42h-44h
DAPI
ELAV
Dcp-1
Merge

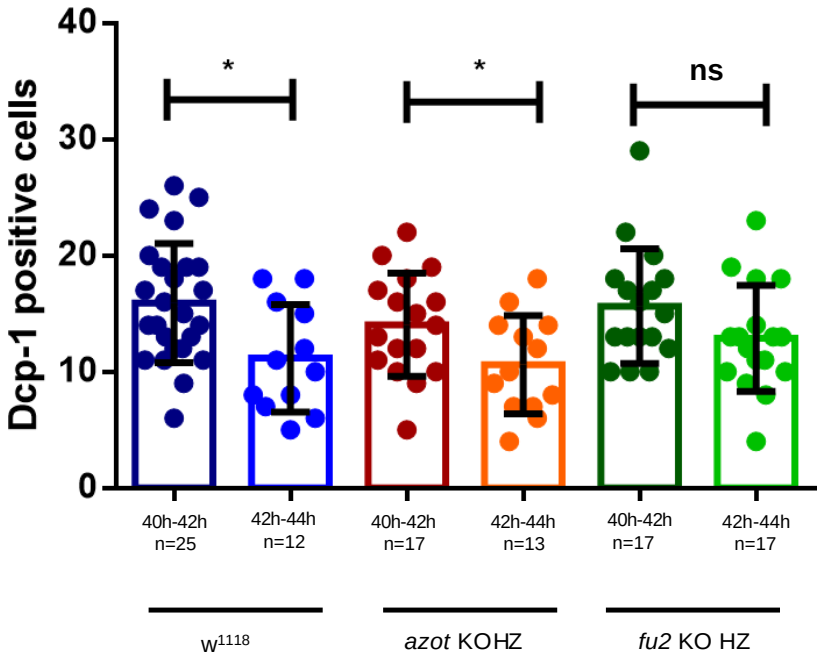

Figure 3.15 – fu2 is not involved in the neuronal culling during pupal stage. Pupal retinas of (A) w^{1118}, (B) azot KO homozygous (azot KO HZ) and (C) fu2 KO homozygous (fu2 KO HZ) from two different timepoints (40-42h and 42-44h APF) stained with DAP (in blue), Dcp-1 (in green) and Elav (in magenta). The white arrows are pointing to the edge of the retinas (regions that were quantified). (D) – Quantification of the number of dying cells (Dcp1 positive cells) in the different genotypes in different timepoints (40-42h APF and 42-44h APF). Each dot corresponds to the mean of three measurements per retina. n - number of retinas analysed per condition; (*)-p≤0.05. ns – not significant.

4 – Discussion

In this project, *fu2* KO stocks were generated using CRISPR-Cas9 system, with the aim of perceiving the role of this gene in different cell competition scenarios. Meanwhile, an experiment using RNAi lines against *fu2* was performed to test if the downregulation of *fu2* (*fu2* knockdown) was sufficient to induce an alteration of cell death in a neurodegenerative context. However, the use of RNAi to study the impact of a gene may not be the adequate strategy. Studies show that the efficiency of distinct RNAi lines may account for different phenotypes – some RNAi lines promote the total degradation of mRNA, which should mimic the KO phenotype, whilst other lines only induces the knockdown of genes. This may complicate the interpretation of results (Kaya-çopur and Schnorrer, 2016). For this reason, *fu2* KO lines were generated, which allows the study of *fu2* in a scenario where this gene is absent.

4.1 – CRISPR-Cas9 technology

Nowadays, CRISPR-Cas9 is widely used to rapidly and efficiently modify endogenous genes in organisms that have been challenging to manipulate genetically (Sander and Joung, 2014). Although it is generally used, CRISPR-Cas9 technique has some limitations. One of them is the cleavage of off-target DNA regions, a limitation common to all nuclease-based genome editing (zinc-finger nucleases, Transcription Activator-Like Effector Nuclease and CRISPR-Cas9 system). This happens due to Cas9 mismatch tolerance - in general, up to three mismatches are tolerated - and to the ratio Cas9/sgRNA (Ran et al., 2013). Note that there is a higher specificity in the final 12 nucleotides (seed sequence) of the sgRNA and in the PAM sequence, which means that if SNPs occur in this core region, the off-target effects are increased (Bassett et al., 2013; Cong et al., 2013; Wang, 2014). In this project, two strategies were performed to generate two independent KO lines.

The first strategy consisted in injecting two sgRNAs to induce the excision of *fu2* coding sequence followed by the DNA repair through NHEJ. This type of DNA repair is error prone and can lead to the insertion or the deletion of sequences (Anton et al., 2018), which may interfere with the regulation of adjacent genes. An initial attempt to induce HDR upon DSB generation promoted by sgRNAs 85/86 and 87/88 was performed, though, when the injected flies were sequenced, no “repair template” was detected in *fu2* locus. This might be due to off-target effect of the sgRNAs – there might have recognized another region of the genome and the “repair template” might have been inserted in that region. The off-target effect hypothesis is strengthened when the phenotype of KO flies is analysed – wings are curved down, which does not occur with the other KO line generated. To validate the off-target hypothesis, a whole genome sequencing should be performed and compared to the *Drosophila* DNA template present in databases. Alternatively, by analysing the progeny of homozygous *fu2* 15.6 KO flies that don’t express the phenotype (normal wings), it is possible to identify if the phenotype is due to off-target effects: if the phenotype is detected in the progeny, then it is not due to off-targets.

For the second strategy, sgRNA target regions (5’HA and 3’HA of gDNA from nos-Cas9 flies) were sequenced to search for possible SNPs, and no mismatch was found, ensuring the recognition between

sgRNAs and target DNA. Furthermore, a deep search in CRISPR Target Finder software (http://flycrispr.molbio.wisc.edu/tools) revealed no off-target regions neither for *fu2* sgRNA -95, nor for *fu2* sgRNA -8. Therefore, the designed sgRNAs were suitable to use for *fu2* KO generation (Figure 2.5).

The amount of DNA injected in the embryos may affect the viability of the embryos, reason why a DNA concentration above 1000ng/µL should be avoided (http://flycrispr.molbio.wisc.edu/protocols/injection). To avoid the injection of two vectors, each of which containing a single sgRNA (performed in the first strategy), for the second strategy, the sequence of both guides (*fu2* sgRNA -95 and *fu2* sgRNA -8) were cloned in the same vector – pCFD5 vector. This vector was created with the purpose of expressing multiple sgRNAs, using transfer RNA (tRNA)–sgRNA expression system existing in rice. In this system, sgRNAs are generated upon tRNA processing. Therefore, from a single precursor RNA transcript, multiple sgRNAs are created. In pCFD5, Cas9 sgRNAs are flanked by *Drosophila* $tRNA^{Gly}$ downstream of a single U6:3 promoter (Port and Bullock, 2016), the strongest promoter in *Drosophila* (Port et al., 2014). For all the reasons mentioned above, this was the more appropriate vector to clone *fu2* sgRNA -95 and *fu2* sgRNA -8.

To flank the “repair template” with homology arms, 5’ and 3’ HA were cloned in pTV3, using specific primers. These primers contained *fu2* sgRNA -95+PAM sequences, upstream 5’HA, and *fu2* sgRNA -8+PAM sequences, downstream 3’HA (Figure 3.3). These fragments are essential for Cas9 to, simultaneously, cut the genome and the vector, avoiding the use of a restriction enzyme to linearize the vector, and reducing this way, the complexity of the injection mixture (Baena-Lopez et al., 2013). The double cut will induce the generation of a linear “repair template”, increasing the possibility of a HDR event. Both HAs must have, in the “repair template”, the PAM sequence mutated, in the 3’ end of 5’HA and in the 5’ end of 3’HA. Otherwise, Cas9 could continuously excise the “repair template” from the genome.

Both vectors (pCFD5 and pTV3) were injected in embryos expressing Cas9 in the germline (nos-Cas9 flies). This stock was chosen since the homology recombination is more efficient if it occurs at the germline level (Baena-Lopez et al., 2013).

The strategy to create *fu2* KO 15.4 proved to be more efficient (efficiency=1%) than the strategy for *fu2* KO 15.6, (efficiency= 0.08%). This might be due to off-target effects induced by sgRNA 85/86 and/or sgRNA87/88, although no off-targets were identified when using CRISPR Target Finder software (http://flycrispr.molbio.wisc.edu/tools). The low efficiency in *fu2* KO 15.6 might also be due to the product generated by the NHEJ DNA repair system. In fact, a study from 2012 shows that, in *Drosophila*, NHEJ in the germline is inhibited, in order to prevent *de novo* mutations. This study outlines the fact that during meiosis, many DSB events occur due to the crossover formation and, in order to prevent the generation of mutations, by NHEJ, HDR is promoted between homologue chromosomes (Joyce et al., 2012).

Although the first strategy for KO generation was not optimized, since *fu2* KO 15.6 was the first KO line generated, all experiments involving a KO in this project were performed using this stock, with the

exception of the recombinant generation. For further studies, *fu2* KO 15.4 will be used, instead of *fu2* KO 15.6.

The generation of the *fu2* KO with concomitant integration of an attP site allows the creation of knock-in lines, where the sequence of interest will be expressed under the endogenous promoter of *fu2*. Concerning the KI generation, the integration vectors with the insertion sequences are already generated and waiting for injection. In these vectors, there was the need to add the 95 nucleotides upstream *fu2* TSS, which were excised along with *fu2* coding sequence upon Cas9 cut. These 95 nucleotides are important to restore the whole regulatory region (5' UTR) of *fu2*, which could otherwise be compromised, altering the post-transcriptional regulation of *fu2* (Bugaut and Balasubramanian, 2012). Two different knock-in lines will be generated: [*fu2 KO, KI lexAp65*] and *[fu2 KO, KI,fu2::mCherry*]. With these knock-in lines, it is possible to address the expression of *fu2* in tissues, as well as the protein subcellular localization. Additionally, using [*fu2 KO, KI lexAp65*] it is possible to control *fu2* in terms of time and place of expression.

When analysing the two KO lines it is verified that both KO are homozygous viable. The fact that flies survive in the absence of *fu2* contradicts the work of Nestor O. Nazario-Yepiz and colleagues (Nazario-Yepiz and Riesgo-Escovar, 2017). In this report, *fu2* mutant alleles are generated by excision of a P-element inserted near the TSS of *fu2*. When this P-element was excised, it created some deletions in *fu2* locus. In this study, all three mutant alleles generated this way are homozygous lethal (Nazario-Yepiz and Riesgo-Escovar, 2017). However, sequencing results failed to reveal any alteration in the gene and mRNA of *fu2* was still detected by semi-quantitative PCR after the P-element excision, which led us to believe that the phenotypic abnormalities verified in this work were not due to *fu2* gene. Probably the P-element was inserted in other region of the genome, inducing deletion of other genes.

Although both KO lines are homozygous viable, the phenotypic analysis revealed that the occurrence of homozygous flies is not according to the mendelian ratio – only 8.22% of the flies resulting from the cross between two *fu2* KO 15.4 heterozygous flies are homozygous. This means that *fu2* locus is being preferentially transmitted to the progeny and, therefore, we can hypothesize that *fu2* gene is important for the correct development of the fly.

4.1.1 – HA-tag generation

Although *fu2*-HA stocks already exist in the lab, this sequence is under the control of *UAS*, which means that *fu2* is not analysed under physiological conditions.

The goal of the *fu2*::3xHA-tag generation was to tag *fu2* in order to study its expression in tissues in normal conditions. However, the strategy used was not successful. The sequencing results (Figure 3.11) revealed the insertion of an unknown sequence. We can exclude that this result is a sequencing artefact, since it was performed multiple times and by different facilities (STABVIDA and GATC). Additionally, the

Integrated DNA Technologies company that synthesized the oligonucleotide confirmed that the oligonucleotide sequence was correct, excluding any issue with the oligonucleotide fragment.

This result might be due to the poor design of sgRNA 87/88. Although no off-target regions were identified for this sgRNA in CRISPR Target Finder software (http://flycrispr.molbio.wisc.edu/tools), it causes a lot of mortality, which is observed by the low efficiency reported in 3xHA-tag generation (0.17%) (chapter 3.2.1) and in *fu2* KO generation using the old guides (0.08%) (chapter 3.1.5). It is possible that the HDR only occurred in one end of the oligo (the 3' end, which explained the insertion of one copy of the HA-tag, the 33 nucleotides restored and the mutated PAM) and an event of NHEJ happened simultaneously to seal the DSB in the 5' end of the oligonucleotide, deleting two copies of the HA-tag.

4.2 – The role of *fu2* in Alzheimer's disease

Previous results from the lab have shown that around 60% of cell death caused by $A\beta_{42}$ overexpression is *fwe*-dependent (Coelho *et al. in preparation*). Since *fu2* was found to be expressed in loser cells (Rhiner et al., 2010), it was decided to test whether *fu2* is required for the *fwe*-dependent cell death. If this is the case, it would be expected that the downregulation of *fu2* was sufficient to change the cell death promoted by $A\beta_{42}$. Indeed, the downregulation of *fu2* using one of the RNAi lines (TRiP line) resulted in different levels of cell death. However, and contrary to expectations, the level of cell death increased when *fu2* was downregulated (Figure 3.12), which may suggest that *fu2* is, in the context of this neurodegenerative disease, playing a protective role, by activating an unknown mechanism that prevents cells to enter apoptosis. On the other hand, it is not possible to conclude this, since the RNAi lines show different results.

The generation of a KO line allow us to clarify the contribution of *fu2* for cell elimination in this disease context. Since transgenic flies carry *UAS*-$A\beta_{42}$ sequence in the second chromosome (the same chromosome as *fu2*), a recombinant line yw hs-flp*; UAS-Aβ42, fu2 {KO, KI-3xpax3::mCherry 15.4}/CyO; MKRS/TM6B was produced* to evaluate the effect of $A\beta_{42}$ in the absence of *fu2*.

4.2.1 – Recombinant generation

To undoubtably evaluate the role of *fu2* in Alzheimer's disease model, the use of the recombinant is crucial. By generating flies with GMR-Gal4 sequence inserted on the first chromosome and the recombinant construct (*UAS-Aβ42, fu2 {KO, KI-3xpax3::mCherry 15.4})* on the second chromosome, it is possible to induce the overexpression of $A\beta_{42}$ in a context where *fu2* is not present. With this experiment it is possible to clarify the data obtained using the RNAi lines.

4.3 – Effect of *fu2* upon neuronal culling

It is known that the supernumerary neurons existing in the periphery of the retinas are eliminated through a *fwe*-dependent mechanism, which requires the expression of fwe^{loseB} (Merino et al., 2013) and that

fu2 is expressed in loser cells (Rhiner et al., 2010). The aim of this experiment was to know if *fu2* played a role in the elimination of neurons during neuronal culling. The results were inconclusive, since the lack of the cell fitness checkpoint (*azot*) did not reveal a significant reduction in cell death when compared to a wild-type retina (w^{1118}).

Since the neuronal culling is a *fwe*-dependent mechanism (Merino et al., 2013), it would be expected that the absence of *azot* (*azot* KO HZ), which impairs the *fwe*-dependent pathway for cell death, resulted in less Dcp-1 positive cells – *hid* would not be expressed and apoptosis would not be triggered (Merino et al., 2015). However, the obtained results showed that the lack of *azot* does not reduce the number of dcp-1 positive cells. This might be due to a staining problem, i. e., some quantified Dcp-1 positive cells may not be addressing dying cells. There are studies showing that caspases may also participate in non-apoptotic cellular events, such as cell cycle regulation and cell migration and differentiation. In the particular case of neurons, studies have shown that, under physiological conditions, the mammalian Caspase-3 (an homologue of Dcp-1) is capable of inducing neuronal cytoskeleton changes, synaptic remodelling and differentiation of glial cells (Harrison et al., 2007). To distinguish the Dcp-1 positive cells ,that are in fact dying cells, from other fates, another type of immunostaining needs to be performed such as Terminal deoxynucleotidyl transferase dUTP nick end labelling (TUNEL) staining. With this staining, labelled dUTPs are added at the 3'-OH ends of single or double strand DNA breaks (Sarkissian et al., 2014). The fragmentation of DNA occurs in a late stage of apoptosis and it is critical for cells to die, which means that TUNEL method only stains late stage apoptotic cells. Thus, it is possible to have Dcp-1 positive and TUNEL negative cells, meaning that these cells are indeed not dying (Wagner et al., 2011).

4.4 – Fu2 may interact with other proteins

Data assessed in flybase, associated Fu2 with two other proteins: Vta1 and CG40228. Vta1 (Vps20-associated 1) protein is related with vesicular trafficking and CG40228 belongs to the transcription elongation factor superfamily (http://flybase.org/). This means that *fu2* could be expressed in loser cells to modify vesicular transportation or the affinity of RNA polymerase II to specific genes. Note however that these experiments were performed *in vitro* and not in *Drosophila*. Therefore, it is not yet possible to confirm the association of Vta1 and CG40228 to Fu2.

4.5 – Conclusion and future work

In this project the molecular tools required to properly addressing the function of *fu2* were generated successfully, allowing the creation of *fu2* KO transgenic flies, which are homozygous viable. Also, two different *fwe*-dependent contexts of cell competition, different from the one where *fu2* was discovered (supercompetition), were used.

To conclude, Figure 4.1 shows a schematic that summarizes the current knowledge of *fu2* function in *fwe*-dependent mechanisms. It is known that, when winner supercompeptitor cells, overexpressing *dMyc*, communicate with loser WT cells, expressing basal levels of *dMyc*, *fwe*-dependent mechanisms will be triggered, leading to the expression of *azot* and, ultimately, to the induction of apoptosis. Fu2 could act to regulate *azot* gene, or it could act in processes upstream of *azot*, such as *fwe* regulation, or downstream of *azot*, such as *hid* regulation.

The role of *fu2* in cell competition may be tissue and context-dependent. Although this thesis couldn't show its influence in neuronal culling or Alzheimer's disease context, it is possible that, apart from supercompetition scenario, *fu2* might be involved in other events of *few*-dependent cell elimination such as the ones promoted by injury and UV irradiation.

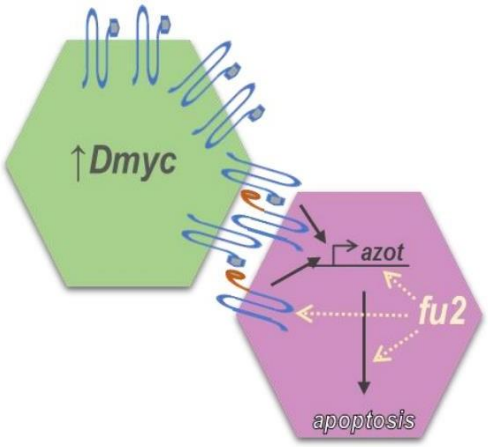

Figure 4.1 – Schematic showing the current working model.

5 – References

Aldaz, S., and Escudero, L.M. (2010). Imaginal discs. Curr. Biol. *20*, 429–431.

Anton, T., Karg, E., and Bultmann, S. (2018). Applications of the CRISPR / Cas system beyond gene editing. 1–10.

Bachmann, A., and Knust, E. (2008). The Use of P-Element Transposons to Generate Transgenic Flies. (Humana Press), pp. 61–77.

Baena-Lopez, L.A., Alexandre, C., Mitchell, A., Pasakarnis, L., and Vincent, J.-P. (2013). Accelerated homologous recombination and subsequent genome modification in Drosophila. Development *140*, 4818–4825.

Bassett, A.R., Tibbit, C., Ponting, C.P., and Liu, J.L. (2013). Highly Efficient Targeted Mutagenesis of Drosophila with the CRISPR/Cas9 System. Cell Rep. *4*, 220–228.

Bondy-Denomy, J., and Davidson, A.R. (2014). To acquire or resist: The complex biological effects of CRISPR-Cas systems. Trends Microbiol. *22*, 218–225.

Brás-Pereira, C., and Moreno, E. (2018). Mechanical cell competition. Curr. Opin. Cell Biol. *51*, 15–21.

Bugaut, A., and Balasubramanian, S. (2012). 5'-UTR RNA G-quadruplexes: translation regulation and targeting. Nucleic Acids Res. *40*, 4727–4741.

Carroll, D. (2014). Genome Engineering with Targetable Nucleases. Annu. Rev. Biochem. *83*, 409–439.

Clavería, C., and Torres, M. (2016). Cell Competition: Mechanisms and Physiological Roles. Annu. Rev. Cell Dev. Biol. *32*, 411–439.

Cong, L., Ran, F.A., Cox, D., Lin, S., Barretto, R., Hsu, P.D., Wu, X., Jiang, W., and Marraffini, L.A. (2013). Multiplex Genome Engineering Using CRISPR/VCas Systems. Science (80-.). *339*, 819–823.

CRISPR Optimal Target Finder website: http://tools.flycrispr.molbio.wisc.edu/targetFinder/ [Acessed: 7-Aug- 2018]

Cutler, T., Sarkar, A., Moran, M., Steffensmeier, A., Puli, O.R., Mancini, G., Tare, M., Gogia, N., and Singh, A. (2015). Drosophila eye model to study neuroprotective role of CREB binding protein (CBP) in Alzheimer's disease. PLoS One *10*, 1–18.

Doublie, S., and Tabor, S. (1998). Crystal structure of a bacteriophage T 7 DNA replication complex at 2. 2 aa resolution. Nature *39*, 251–258.

Elliott, D. a, and Brand, A.H. (2008). The GAL4 system : a versatile system for the expression of genes. Methods Mol. Biol. *420*, 79–95.

Fernandez-Funez, P., de Mena, L., and Rincon-Limas, D.E. (2015). Modeling the complex pathology of Alzheimer's disease in Drosophila. Exp. Neurol. *274*, 58–71.

Flagg, R.O. (1979). Carolina Drosophila Manual. Carolina Biol. Supply Co. 36. Flybase website: http://flybase.org/ [Accessed: 15-Sept-2018]

Gaj, T., Gersbach, C.A., and Barbas, C.F. (2013). ZFN, TALEN, and CRISPR/Cas-based methods for genome engineering. Trends Biotechnol. *31*, 397–405.

Gogna, R., Shee, K., and Moreno, E. (2015). Cell Competition During Growth and Regeneration. Annu. Rev. Genet. *49*, 697–718.

Di Gregorio, A., Bowling, S., and Rodriguez, T.A. (2016). Cell Competition and Its Role in the Regulation of Cell Fitness from Development to Cancer. Dev. Cell *38*, 621–634.

Hales, K.G., Korey, C.A., Larracuente, A.M., and Roberts, D.M. (2015). Genetics on the fly: A primer on the drosophila model system. Genetics *201*, 815–842.

Harrison, J.F., Rinne, M.L., Kelley, M.R., Druzhyna, N.M., Wilson, G.L., and Ledoux, S.P. (2007). Altering DNA base excision repair: use of nuclear and mitochondrial-targeted N-methylpurine DNA glycosylase to sensitize astroglia to chemotherapeutic agents. Glia *55*, 1416–1425.

Haynie, J.L., and Bryant, P.J. (1986). Development of the eye-antenna imaginal disc and morphogenesis of the adult head in Drosophila melanogaster. J. Exp. Zool. *237*, 293–308.

Huang, J., Zhou, W., Dong, W., Watson, A.M., and Hong, Y. (2009). From the Cover: Directed, efficient, and versatile modifications of the Drosophila genome by genomic engineering. Proc. Natl. Acad. Sci. U. S. A. *106*, 8284–8289.

Huang, L.O., Labbe, A., and Infante-Rivard, C. (2013). Transmission ratio distortion: Review of concept and implications for genetic association studies. Hum. Genet. *132*, 245–263.

Jasin, M., Haber, J.E., Program, B., Basic, R., and Sciences, M. (2017). HHS Public Access. 6–16.

Jennings, B.H. (2011). Drosophila - a versatile model in biology & medicine. Mater. Today *14*, 190–195.

Joyce, E.F., Paul, A., Chen, K.E., Tanneti, N., and McKim, K.S. (2012). Multiple barriers to nonhomologous DNA end joining during meiosis in Drosophila. Genetics *191*, 739–746.

Kaya-çopur, A., and Schnorrer, F. (2016). Drosophila. *1478*.

Kilpatrick S.T., Krebs J. E., G.E.S. (2014). Eukaryotic Transcription Regulation.

Korbie, D.J., and Mattick, J.S. (2008). Touchdown PCR for increased specificity and sensitivity in PCR amplification. Nat. Protoc. *3*, 1452–1456.

de la Fuente-Núñez, C., and Lu, T.K. (2017). CRISPR-Cas9 technology: applications in genome engineering, development of sequence-specific antimicrobials, and future prospects. Integr. Biol. *9*, 109–122.

LaFountaine, J.S., Fathe, K., and Smyth, H.D.C. (2015). Delivery and therapeutic applications of gene editing technologies ZFNs, TALENs, and CRISPR/Cas9. Int. J. Pharm. *494*, 180–194.

Laity, J.H., Lee, B.M., and Wright, P.E. (2001). Zinc finger proteins: New insights into structural and functional diversity. Curr. Opin. Struct. Biol. *11*, 39–46.

Lambing, C., Franklin, F.C.H., and Wang, C.-J.R. (2017). Understanding and Manipulating Meiotic Recombination in Plants. Plant Physiol. *173*, 1530–1542.

Lenz, S., Karsten, P., Schulz, J.B., and Voigt, A. (2013). Drosophila as a screening tool to study human neurodegenerative diseases. J. Neurochem. *127*, 453–460.

Levayer, R., and Moreno, E. (2016). How to be in a good shape? The influence of clone morphology on cell competition. Commun. Integr. Biol. *9*, 1–4.

Li, H., Beckman, K.A., Pessino, V., Huang, B., and Weissman, J.S. (2017). Design and specificity of long ssDNA donors for CRISPR-based knock-in.

Lolo, F.N., Tintó, S.C., and Moreno, E. (2013). How winner cells cause the demise of loser cells: Cell competition causes apoptosis of suboptimal cells: Their dregs are removed by hemocytes, thus preserving tissue homeostasis. BioEssays *35*, 348–353.

Luther, D.C., Lee, Y.W., Nagaraj, H., Scaletti, F., and Rotello, V.M. (2018). Delivery Approaches for CRISPR/Cas9 Therapeutics *In Vivo* : Advances and Challenges. Expert Opin. Drug Deliv.

17425247.2018.1517746.

Ma, Y., Zhang, L., and Huang, X. (2014). Genome modification by CRISPR/Cas9. FEBS J. *281*, 5186–5193.

Marygold, S.J., Roote, J., Reuter, G., Lambertsson, A., Ashburner, M., Millburn, G.H., Harrison, P.M., Yu, Z., Kenmochi, N., Kaufman, T.C., et al. (2007). The ribosomal protein genes and Minute loci of Drosophila melanogaster. Genome Biol. *8*.

Matsumoto, T., Koshii, Y., Sakane, K., Murakawa, T., Hirayama, Y., Yoshida, H., Kurokawa, M., Tamura, Y., Nagai, T., and Kawase, I. (2013). A novel approach to automated genotyping of Mycobacterium tuberculosis using a panel of 15 MIRU VNTRs. J. Microbiol. Methods *93*, 239–241.

McKim, K.S., and Hayashi-Hagihara, A. (1998). mei-W68 in Drosophila melanogaster encodes a Spo11 homolog: Evidence that the mechanism for initiating meiotic recombination is conserved. Genes Dev. *12*, 2932–2942.

mendelian ratio. (n.d.) Farlex Partner Medical Dictionary. (2012). Retrieved September 22 2018 from https://medical-dictionary.thefreedictionary.com/mendelian+ratio

Merino, M.M., Rhiner, C., Portela, M., and Moreno, E. (2013). "Fitness fingerprints" mediate physiological culling of unwanted neurons in drosophila. Curr. Biol. *23*, 1300–1309.

Merino, M.M., Rhiner, C., Lopez-Gay, J.M., Buechel, D., Hauert, B., and Moreno, E. (2015). Elimination of unfit cells maintains tissue health and prolongs lifespan. Cell *160*, 461–476.

Merino, M.M., Levayer, R., and Moreno, E. (2016). Survival of the Fittest: Essential Roles of Cell Competition in Development, Aging, and Cancer. Trends Cell Biol. *26*, 776–788.

Mhatre, S.D., Satyasi, V., Killen, M., Paddock, B.E., Moir, R.D., Saunders, A.J., and Marenda, D.R. (2014). Synaptic abnormalities in a Drosophila model of Alzheimer's disease. Dis. Model. Mech. *7*, 373–385.

Morata, G., and Ballesteros-Arias, L. (2015). Cell competition, apoptosis and tumour development. Int. J. Dev. Biol. *59*, 79–86.

Morata, G., and Ripoll, P. (1975). Minutes: Mutants of Drosophila autonomously affecting cell division rate. Dev. Biol. *42*, 211–221.

Moreno, E. (2008). Is cell competition relevant to cancer? Nat. Rev. Cancer *8*, 141–147.

Moreno, E., and Rhiner, C. (2014). Darwin's multicellularity: From neurotrophic theories and cell competition to fitness fingerprints. Curr. Opin. Cell Biol. *31*, 16–22.

Moreno, E., Basler, K., and Morata, G. (2002). Cells compete for decapentaplegic survival factor to prevent apoptosis in Drosophila wing development. Nature *416*, 755–759.

Moreno, E., Fernandez-Marrero, Y., Meyer, P., and Rhiner, C. (2015). Brain regeneration in Drosophila involves comparison of neuronal fitness. Curr. Biol. *25*, 955–963.

Naylor, L.H. (1999). Reporter gene technology: the future looks bright. Biochem. Pharmacol. *58*, 749–757.

Nazario-Yepiz, N.O., and Riesgo-Escovar, J.R. (2017). piragua encodes a zinc finger protein required for development in Drosophila. Mech. Dev. *144*, 171–181.

Newman, E.A., Lu, F., Bashllari, D., Wang, L., Opipari, A.W., and Castle, V.P. (2015). Alternative NHEJ Pathway Components Are Therapeutic Targets in High-Risk Neuroblastoma. Mol. Cancer Res. *13*, 470–

482.

Nuclease, R.C., Gratz, S.J., Cummings, A.M., Nguyen, J.N., Hamm, D.C., Donohue, L.K., Harrison, M.M., Wildonger, J., and Connor-giles, K.M.O. (2013). Genome Engineering of Drosophila with the CRISPR. *194*, 1029–1035.

Özel, M.N., Langen, M., Hassan, B.A., and Hiesinger, P.R. (2015). Filopodial dynamics and growth cone stabilization in Drosophila visual circuit development. Elife *4*, 1–21.

Port, F., and Bullock, S.L. (2016). Augmenting CRISPR applications in Drosophila with tRNA-flanked sgRNAs. Nat. Methods *13*, 852–854.

Port, F., Chen, H.-M., Lee, T., and Bullock, S.L. (2014). Optimized CRISPR/Cas tools for efficient germline and somatic genome engineering in Drosophila. Proc. Natl. Acad. Sci. *111*, E2967–E2976.

Portela, M., Casas-Tinto, S., Rhiner, C., L??pez-Gay, J.M., Dom??nguez, O., Soldini, D., and Moreno, E. (2010). Drosophila SPARC is a self-protective signal expressed by loser cells during cell competition. Dev. Cell *19*, 562–573.

Prüßing, K., Voigt, A., and Schulz, J.B. (2013). Drosophila melanogaster as a model organism for Alzheimer ’s disease. Mol. Neurodegener. *8*.

Ran, F.A., Hsu, P.D., Wright, J., Agarwala, V., Scott, D.A., and Zhang, F. (2013). Genome engineering using the CRISPR-Cas9 system. Nat. Protoc. *8*, 2281–2308.

Ready, D.F., Hanson, T.E., and Benzer, S. (1976). Development of the Drosophila retina, a neurocrystalline lattice. Dev. Biol. *53*, 217–240.

Rhiner, C., López-Gay, J.M., Soldini, D., Casas-Tinto, S., Martín, F.A., Lombardía, L., and Moreno, E. (2010). Flower forms an extracellular code that reveals the fitness of a cell to its neighbors in Drosophila. Dev. Cell *18*, 985–998.

Ribeiro, L.F., Ribeiro, L.F.C., Barreto, M.Q., and Ward, R.J. (2018). Protein Engineering Strategies to Expand CRISPR-Cas9 Applications. Int. J. Genomics *2018*, 1–12.

Roote, J., and Prokop, a (2013). How to design a genetic mating sheme: a basic training package for Drosophila genetics. Roote+Prokop-SupplMat-1v3.3.Pdf *Light vers*, 1–22.

Sander, J.D., and Joung, J.K. (2014). CRISPR-Cas systems for editing, regulating and targeting genomes. Nat. Biotechnol. *32*, 347–350.

Sarkissian, T., Timmons, A., Arya, R., Abdelwahid, E., and White, K. (2014). Detecting apoptosis in Drosophila tissues and cells. Methods *68*, 89–96.

Singh, A., and Kango-Singh, M. (2013). Molecular genetics of axial patterning, growth and disease in the drosophila eye.

Sternberg, S.H., and Doudna, J.A. (2015). Expanding the Biologist’s Toolkit with CRISPR-Cas9. Mol. Cell *58*, 568–574.

Tettweiler, G., and Lasko, P. (2007). Investigating Translation Initiation Using Drosophila Molecular Genetics (Elsevier Masson SAS).

Tomlinson, A., and Ready, D.F. (1987). Neuronal differentiation in the Drosophila ommatidium. Dev. Biol. *120*, 366–376.

Tyler, M.S. (2000). Developmental Biology, A Guide for Experimental Study. Dev. Biol. A Guid. Exp. Study 85–106.

Vincent, J.-P., Kolahgar, G., Gagliardi, M., and Piddini, E. (2011). Steep differences in wingless signaling trigger Myc-independent competitive cell interactions. Dev. Cell *21*, 366–374.
Wagner, D.C., Riegelsberger, U.M., Michalk, S., Härtig, W., Kranz, A., and Boltze, J. (2011). Cleaved caspase-3 expression after experimental stroke exhibits different phenotypes and is predominantly non-apoptotic. Brain Res. *1381*, 237–242.
Wang, T. (2014). Genetic Screens in Human Cells Using. *80*, 80–85.
Zhang, F., Wen, Y., and Guo, X. (2016). CRISPR / Cas9 for genome editing : Progress , implications and challenges CRISPR / Cas9 for genome editing : progress , implications and challenges. 39–46.

6 – Supplementary data

6.1 – sgRNA sequences

sgRNA sequences used to perform the first strategy:

sgRNA 85/86: 5’ – ACATAGGTACGCATCAATTA – 3’

sgRNA 87/88: 5’ – GTTTAATAAGCTTAGTTGAT – 3’

sgRNA sequences used to perform the second strategy:

fu2 sgRNA -95: 5’ – AAATAAAACGCGTTGGTCAA – 3’

fu2 sgRNA -8: 5’ – CTACAGCGAGACTCGTCCCG – 3’

6.2 – pCFD5 vector

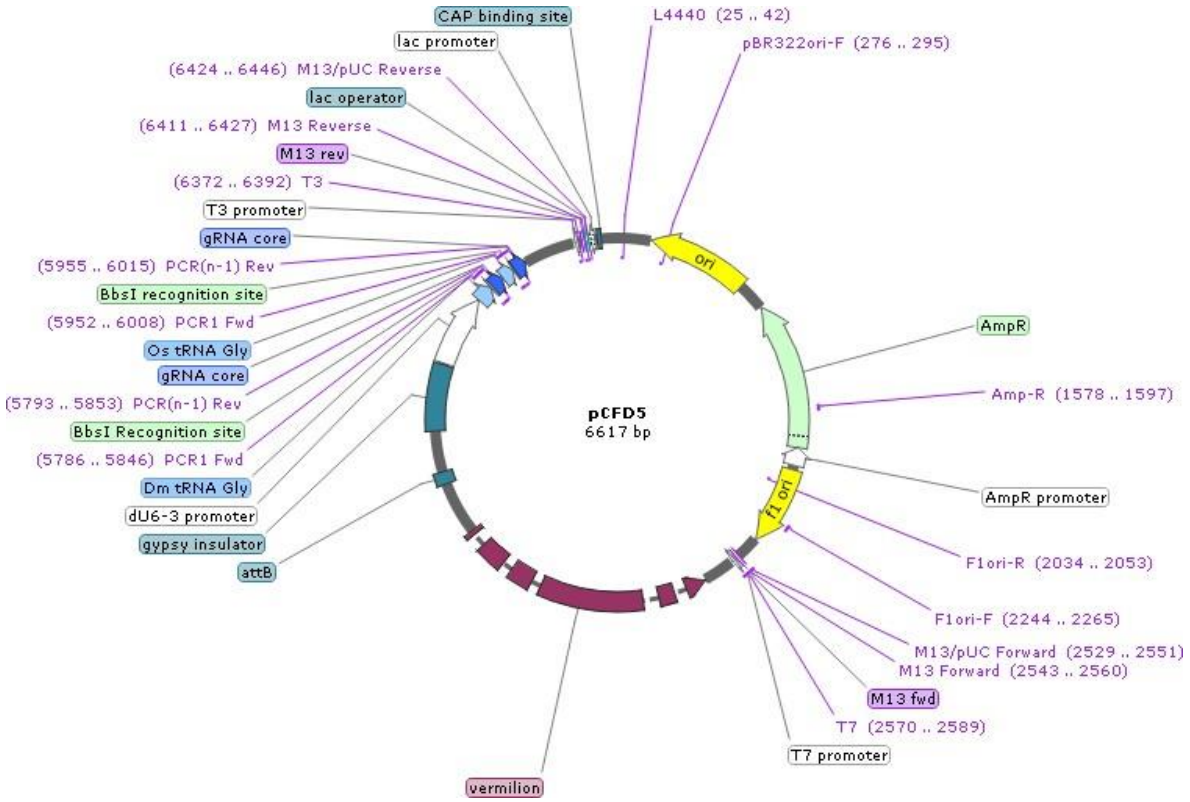

Figure 6.1 – Schematic of pCFD5 vector, used to clone fu2 sgRNA -95 and fu2 sgRNA -8.

6.3 – pCR-Blunt-II-TOPO vector

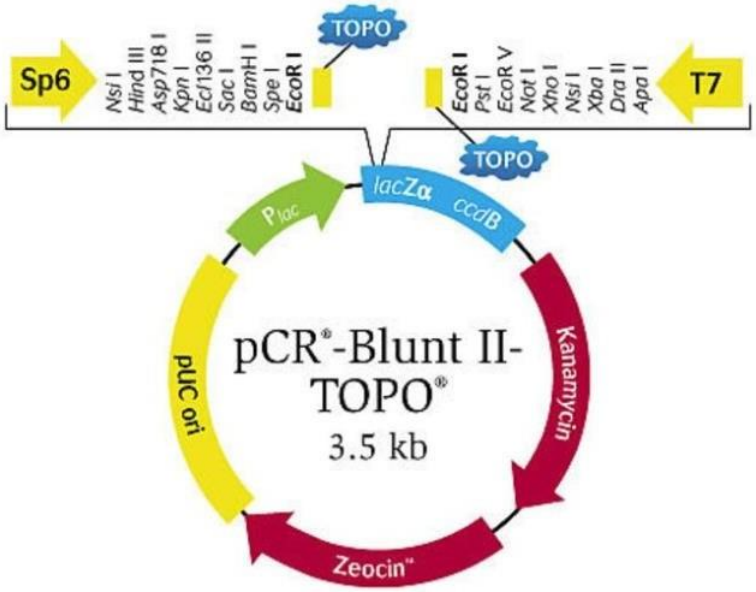

Figure 6.2 – Schematic of pCR-Blunt II-TOPO vector, used as an intermediate vector for 5'HA and 3'HA cloning.

6.4 – pTV3 vector

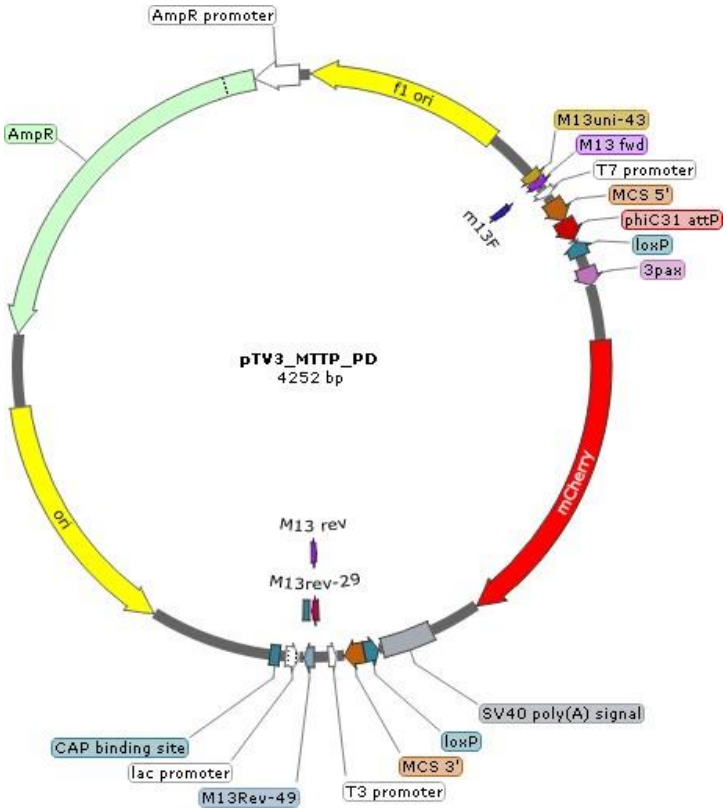

Figure 6.3 – Schematic of pTV3 vector, used to clone 5'HA and 3'HA.

6.5 – Fly food recipe

Table 6.1 – Recipe used to produce fly food and quantities of each ingredient.

Vienna Recipe	Quantities (per liter of H_2O)
Barley Malt Syrup (Próvida)	80g
Beetroot Syrup (Grafschafter)	22g
Agar (NZYTech)	8g
Biological Corn flour (Próvida)	80g
Soya fluor (A. Centazzi)	10g
Instant Yeast (Saf-instant, Lesaffre)	18g
Propionic acid (Argos)	8mL
15% Niapagin (Tegosept, Dutscher UK) in 96% EtOH	12mL